Very recently, Kondapalli, C. *et al.* reported that PINK1 directly phosphorylates Parkin at Ser65 in the Ubl domain[18]. However, the extent and consequences of Parkin phosphorylation by PINK1 in mitochondrial regulation are still not fully understood.

To address this issue, we attempted to independently monitor and compare the phosphorylation status of Parkin in wild-type and *PINK1*-deficient cells, thereby excluding the possibility of phosphorylations by uncharacterised kinases other than PINK1[30]. Here, we also report that Parkin is demonstrably phosphorylated at Ser65 in a PINK1-dependent manner. Furthermore, we show that this phosphorylation event is implicated in the regulation of mitochondrial translocation of Parkin and the subsequent degradation of mitochondrial surface proteins during mitophagy.

Results

Parkin is phosphorylated upon depolarisation in $\Delta\Psi$m. We used [^{32}P] orthophosphate to metabolically label mouse embryonic fibroblasts (MEFs) derived from *PINK1* deficient mice, in which HA-tagged Parkin together with FLAG-tagged wild-type or kinase-dead forms (triple mutant with K219A, D362A and D384A) of PINK1 were virally introduced (hereafter referred to as "PINK1-FLAG WT" or "KD/HA-Parkin/*PINK1*$^{-/-}$" MEFs) and then induced Parkin-mediated mitophagy via treatment with the protonophore carbonyl cyanide *m*-chlorophenyl hydrazone (CCCP). As shown in Figure 1a, Parkin was specifically phosphorylated in CCCP-treated PINK1-FLAG WT/HA-Parkin/*PINK1*$^{-/-}$ MEFs, but not in PINK1-FLAG KD/HA-Parkin/*PINK1*$^{-/-}$ MEFs. Phos-tag Western blotting, in which phosphorylated proteins appear as slower migrating bands[28], revealed that Parkin was phosphorylated within 10 min following CCCP treatment (Fig. 1b). Phosphorylation of Parkin reached its maximum level approximately 40 min after CCCP treatment and was sustained at least until 6 hr (Supplementary Fig. S1). Under these conditions, slower migrating bands of PINK1 also appeared, which very likely reflects the autophosphorylation of PINK1 when activated (Fig. 1b)[18]. The suppression of PINK1 accumulation by RNA interference suggested that$\Delta\Psi$m depolarisation-dependent activation of PINK1 along with PINK1 accumulation is a key element for Parkin phosphorylation (Fig. 1c). Every PINK1 deletion and pathogenic mutant we tested failed to stimulate Parkin phosphorylation effectively, strongly suggesting that intact PINK1 is required for this action (Fig. 1d and e). Importantly, human fibroblasts from a patient with *PINK1*-linked parkinsonism also lacked the activity to phosphorylate Parkin (Fig. 1f). The phosphorylated Parkin disappeared within 30 min during the recovery of $\Delta\Psi$m depolarisation by the removal of CCCP from the culture medium (Fig. 1g). Further analysis using phosphatase and proteasome inhibitors suggested that phosphorylated Parkin is at least partly degraded by proteasomal activity in the mitochondria (Supplementary Fig. S2).

Phosphorylation of Ser65 in the Parkin Ubl domain primes the mitochondrial translocation of Parkin. To determine which residue(s) of Parkin are phosphorylated, we immunopurified HA-tagged Parkin from PINK1-FLAG WT or KD/HA-Parkin/*PINK1*$^{-/-}$ MEFs treated with or without CCCP and performed mass spectrometric analysis for phospho-peptides (Supplementary Fig. S3). Although Phos-tag Western blotting of Parkin mainly detected a single band shift, which represents a single phospho-modification, the mass spectrometric analysis identified Ser9 or Ser10 and Ser65, Ser101 and Ser198 as phosphorylated residues of Parkin. Among these residues, only Ser65 phosphorylation increased (33-fold) in CCCP-treated PINK1-FLAG WT/HA-Parkin/*PINK1*$^{-/-}$ MEFs (Supplementary Fig. S3). Phos-tag Western blotting with mutant forms of Parkin, in which the identified phospho-serine residues are replaced with alanine, revealed that the band shift represents Ser65 phosphorylation (Fig. 2a). An *in vitro* kinase assay with recombinant insect PINK1, which has marked kinase activity[28], strongly suggested that PINK1 directly phosphorylates Parkin at Ser65 (Supplementary Fig. S4). The Ser65 residue lies in the Ubl domain and is highly conserved from human to *Drosophila* (Fig. 2b). We next examined whether phosphorylation of Ser65 is required for Parkin-mediated mitophagy. GFP-tagged Parkin WT, which was localised both in the cytoplasm and in the nuclei of mock (DMSO)-treated cells (0 hr, Fig. 2c and d), was translocated to the mitochondria and induced the perinuclear aggregation of mitochondria 2 hr after CCCP treatment, as previously reported (2 hr, Fig. 2c and d)[17,23]. Replacement of Ser65 with alanine (S65A) did not affect the subcellular localisation of Parkin in mock-treated cells when compared with that of GFP-Parkin WT (0 hr, Fig. 2c and d). However, GFP-Parkin S65A almost completely inhibited the mitochondrial translocation of Parkin and the perinuclear rearrangement of mitochondria 0.5 hr after CCCP treatment (0.5 hr, Fig. 2c and d) and showed delayed translocation in 2 hr (2 hr, Fig. 2c and d). The expression of a putative phosphomimetic Parkin S65E also showed a subcellular localisation similar to that of GFP-Parkin WT in both DMSO- and CCCP-treated cells (Fig. 2c). However, GFP-Parkin S65E exhibited a mild translocation defect, suggesting that S65E does not fully mimic the phosphorylated Ser65 (Fig. 2d).

Parkin Ser65 phosphorylation is not sufficient for mitochondrial translocation upon depolarisation of $\Delta\Psi$m. As PINK1-mediated Ser65 phosphorylation appeared to be required for efficient translocation of Parkin, we next examined whether well-characterised pathogenic Parkin mutants were subjected to phosphorylation upon CCCP treatment. In this experiment, we used three kinds of Parkin mutants based on the previous and current studies (Supplementary Fig. S5)[17,22,23]. The first group, V15M, P37L, R42P and A46P, had intact or weakly impaired mitochondrial translocation activity. The second group, T415N and G430D, had mildly impaired translocation activity. The third group, K161N, K221N and T240R, almost completely lacked translocation activity (Fig. 3a). Surprisingly, all of the mutants possessed comparable phosphorylation efficiencies to those of WT (Fig. 3b). This result suggests that Ser65 phosphorylation is not sufficient for the mitochondrial translocation of Parkin.

Biochemical fractionation of endogenous Parkin from SH-SY5Y cells detected only the phosphorylated form of Parkin in the mitochondrial fraction upon CCCP treatment (Fig. 3c), which strongly suggests that phosphorylation of Parkin is required for mitochondrial translocation. There was a slight difference in the gel mobility of phosphorylated Parkin between the cytosolic and the mitochondrial fractions and between CCCP-treated periods of time. These differences very likely reflect differences in the complexity of the contents of each fraction rather than in the phosphorylation status of Parkin because a single shifted band appears in the mixed fractions (Mito + Cyto in Fig. 3c; CCCP 30 min + 60 min in Supplementary Fig. S6).

Effect of Parkin Ser65 phosphorylation on the autophagic reaction. We next examined whether Ser65 phosphorylation is required for the subsequent autophagic reaction, in which various ubiquitin-proteasome- and autophagy-related proteins are involved, including the 26S proteasome, p97/VCP, p62/SQSTM1, LC3, ATG5 and ATG7[22,23,31–35]. Parkin has been reported to be involved in the ubiquitin-proteasome-dependent degradation of a variety of mitochondrial outer membrane proteins, including Mitofusin1 (Mfn1)[32], Mfn2[32], Miro1[36,37], Miro2[37], VDAC1[22] and Tom20[31]. Degradation of Mfn1, VDAC1 and Tom20 at the mitochondrial outer membrane was observed in PINK1 WT/GFP-Parkin/*PINK1*$^{-/-}$ MEFs 1 to 4 hr after CCCP treatment (Fig. 4a). While GFP-Parkin harbouring S65A or S65E mutations was also capable of inducing Mfn1, VDAC1 and Tom20 degradation, the efficiency was impaired, especially in Mfn1 and VDAC1 (Fig. 4a). Long-term time course analysis revealed that in cells expressing Parkin with S65A or S65E mutations, Mfn1 and VDAC1 cannot be degraded effectively, and the mitochondrial outer membrane was likely more intact as indicated by the sustained

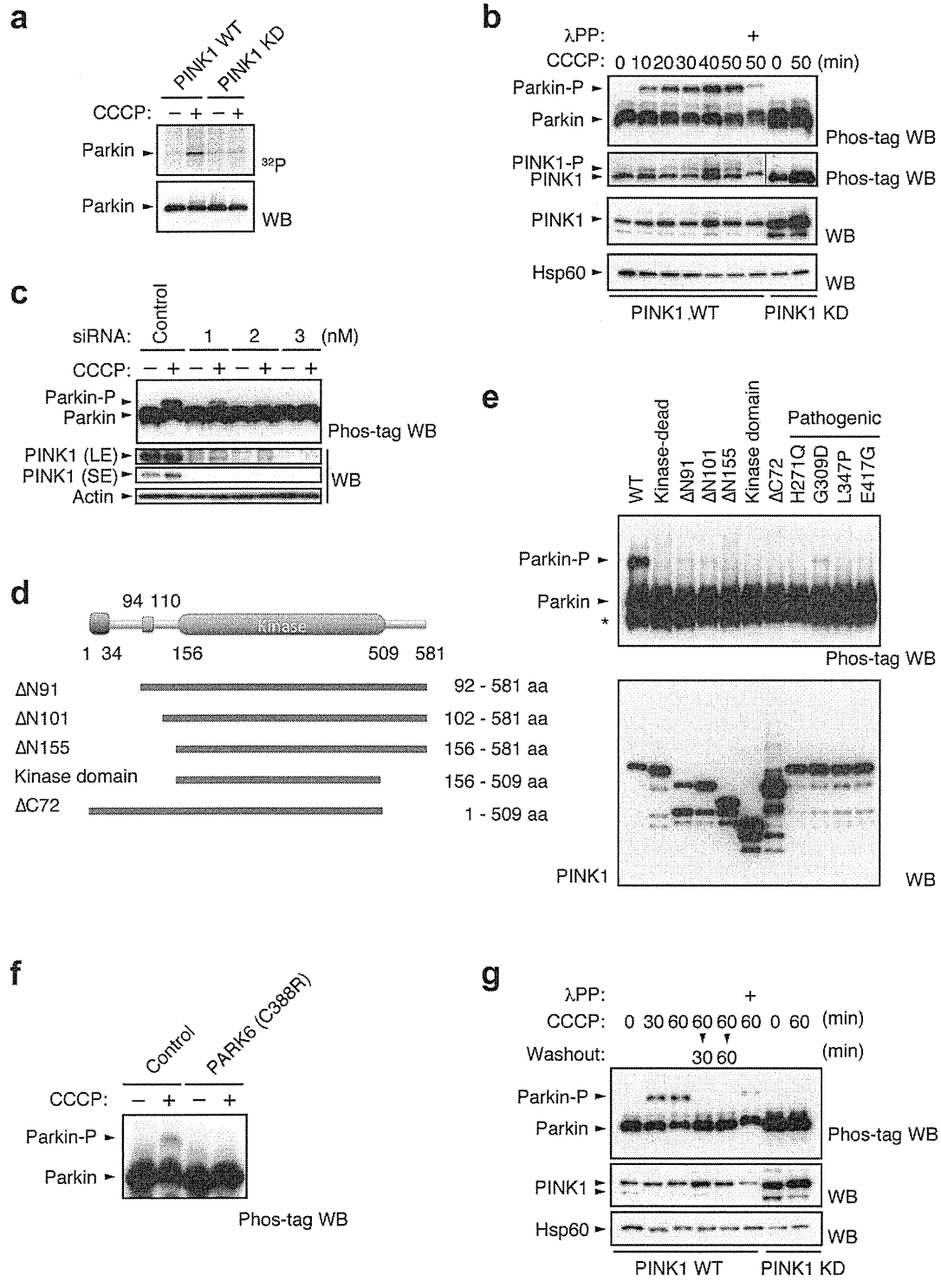

Figure 1 | PINK1-dependent phosphorylation of Parkin *in vivo*. (a) PINK1-FLAG WT or KD/HA-Parkin/*PINK1*$^{-/-}$ MEFs were labelled with [^{32}P] orthophosphate and treated with 30 μM CCCP for 1.5 hr. Phosphorylated Parkin was detected by autoradiography (^{32}P). Immunoprecipitated HA-Parkin was detected by Western blotting (WB) with anti-Parkin. (b) PINK1-FLAG WT or KD/HA-Parkin/*PINK1*$^{-/-}$ MEFs were treated with or without 30 μM CCCP for the indicated periods of time. Cell lysate was subsequently separated on a Phos-tag gel, followed by WB with anti-PINK1 or anti-Parkin antibodies (Phos-tag WB). Phosphorylated bands of Parkin and PINK1 were confirmed by their disappearance with lambda protein phosphatase (λPP) treatment. Mitochondrial Hsp60 was used as a loading control. (c) Suppression of endogenous PINK1 expression inhibits Parkin phosphorylation. HeLa cells stably expressing non-tagged Parkin were treated with the indicated concentrations of stealth siRNA duplex against PINK1 (Invitrogen) with or without 10 μM CCCP for 1 hr. Long- (LE) and short-exposure (SE) blot signals for PINK1 were shown. Actin was used as a loading control. (d) Truncated PINK1 mutants used in this study. Putative mitochondria-targeting sequence, 1–34 aa; transmembrane domain, 94–110 aa; kinase domain, 156–509 aa. (e) Full-length PINK1 is required for Parkin phosphorylation. *PINK1*$^{-/-}$ MEFs stably expressing non-tagged Parkin were transfected with various PINK1 constructs with C-terminal FLAG-tags. PINK1 expression was confirmed with anti-FLAG-HRP. (f) Human fibroblasts from a normal control and a *PARK6* case with a homozygous C388R mutation[44] were transfected with Parkin and were treated with or without 30 μM CCCP for 1 hr. (g) Cells treated with CCCP up to 60 min as in (b) were further incubated with fresh culture medium without CCCP for the indicated periods of time (Washout).

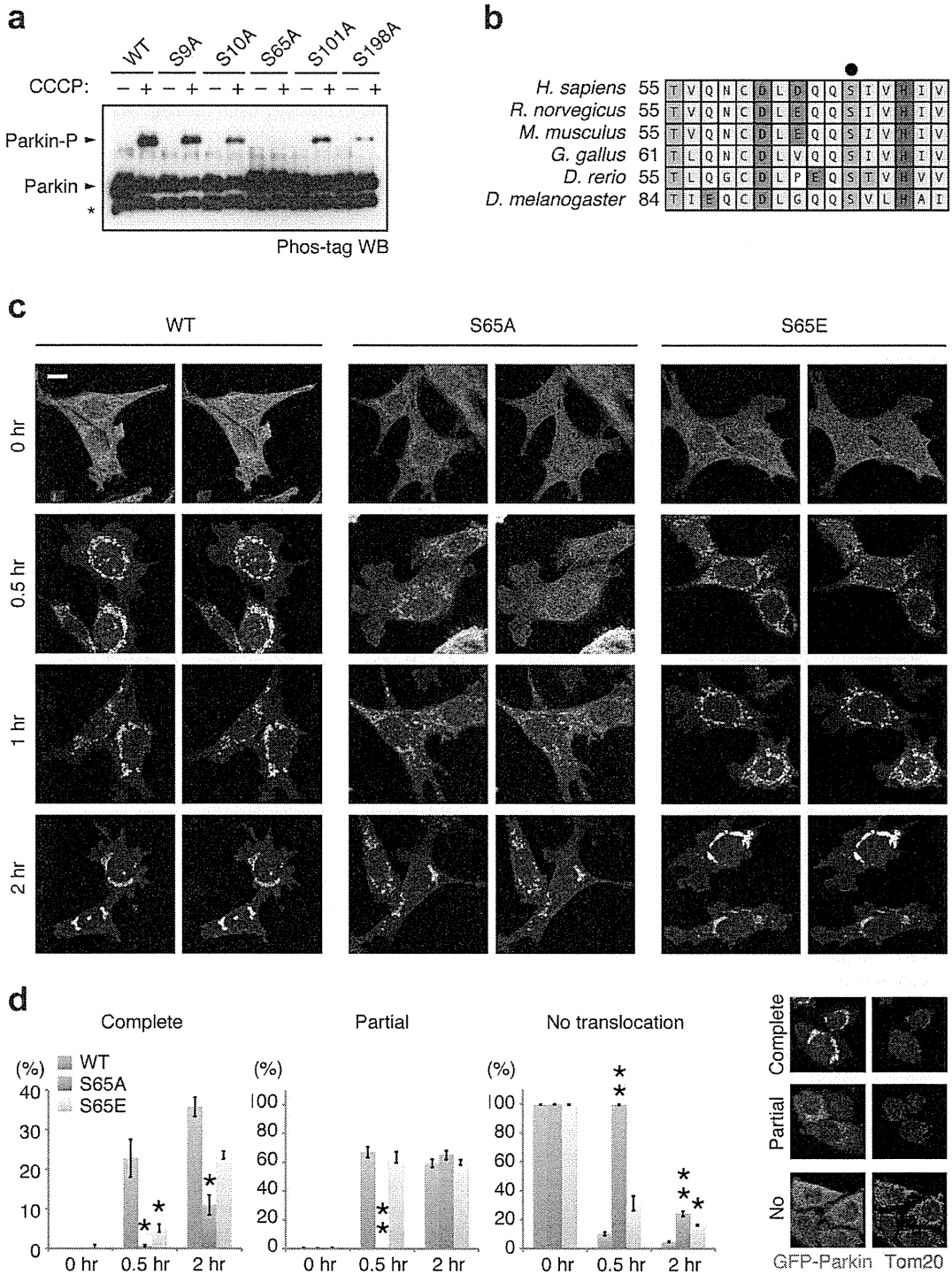

Figure 2 | Ser65 in the Ubl domain of Parkin is phosphorylated upon depolarisation of $\Delta\Psi$m. (a) Phos-tag Western blotting detected phosphorylation of Ser65. HeLa cells were transiently transfected with Parkin WT and a series of alanine mutants for the candidate phospho-residues followed by treatment with or without 20 μM CCCP for 1 hr. Cell lysates were analysed by Phos-tag Western blotting. An asterisk indicates degraded Parkin. (b) Alignment of the amino acid sequences surrounding Ser65 (marked by a black dot) from a variety of animal species. The numbers on the left correspond to the residue numbers of Parkin proteins. (c) Introduction of the S65A mutation delayed Parkin translocation to the depolarised mitochondria in PINK1 WT/GFP-Parkin/*PINK1*$^{-/-}$ MEFs. Cells retrovirally introduced with GFP-Parkin WT or its phospho-mutants (S65A and S65E) were treated with or without 30 μM CCCP for the indicated periods of time. GFP-Parkin and mitochondria were visualised with anti-GFP (green) and anti-Tom20 (red), respectively. Parkin signals are also shown as monochrome images. Scale bar = 10 μm. (d) Mitochondrial translocation efficiency of Parkin mutants. PINK1 WT/*PINK1*$^{-/-}$ MEFs stably expressing GFP-Parkin WT, S65A or S65E were treated as in (c). Cells expressing GFP-Parkin perfectly overlapped (Complete, examples are shown on the right), partially overlapped (Partial) or non-overlapped (No) with the Tom20 signal were counted. The data represent means ± SE from three experiments (n = 99–143 cells in each). ** $p < 0.01$, * $p < 0.05$ *vs.* WT at each time point.

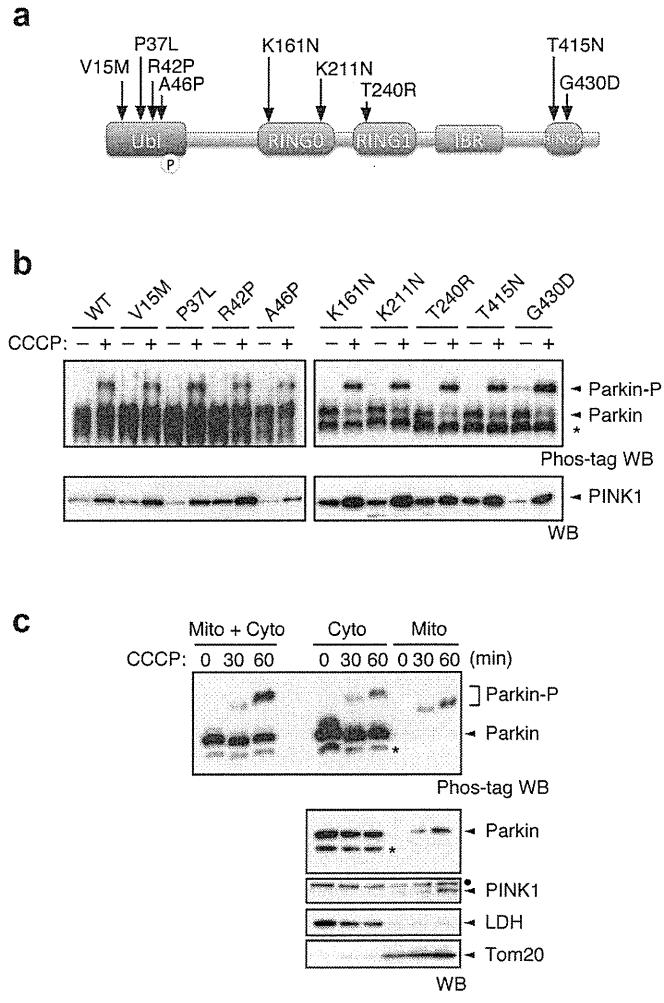

Figure 3 | Pathogenic mutants of Parkin are subjected to Ser65 phosphorylation. (a) Diagram of Parkin protein illustrating the pathogenic mutants used in this study. The Ser65 residue in the Ubl domain is shown as a yellow circle. RING, Ring-finger motif; IBR, in-between-Ring fingers domain. (b) Phos-tag Western blotting for Parkin and Western blotting for PINK1 were performed using Parkin WT and a series of pathogenic mutants as shown in Figure 2a. (c) Endogenous Parkin was also phosphorylated in SH-SY5Y cells after CCCP treatment. Post-nuclear cell lysates from SH-SY5Y cells treated with or without 10 μM CCCP for 30 and 60 min were fractionated into mitochondria-rich (Mito) and cytosolic (Cyto) fractions. These two fractions and their combination (Mito + Cyto) were subjected to Phos-tag or normal Western blotting analyses. Endogenous PINK1 was fractionated in the Mito fraction, as previously reported[45]. Lactate dehydrogenase (LDH) and Tom20 were used as cytosolic and mitochondrial marker proteins, respectively. Asterisks: putative cleaved Parkin; dots: non-specific bands.

accumulation of PINK1 (Fig. 4b). The impaired degradation cannot be explained simply by the delayed translocation of Parkin mutants because both mutants completed the mitochondrial translocation by the 6 hr time-point (data not shown and see Fig. 4c). In contrast, the profiles of Parkin expression and autoubiquitination in Parkin S65A- or S65E-expressing cells were comparable with those of WT (Fig. 4b). We also examined whether Ser65 mutations affect the accumulation of proteasome (Fig. 4c) and p62 (Supplementary Fig. S7) at the mitochondria during mitophagy via the immunostaining of the proteasome subunit alpha type 7 (α7) and p62. However, there was no evidence that Ser65 mutations inhibit or delay the recruitment of proteasome and p62 to the mitochondria. Finally, we tested whether the Parkin Ubl domain itself is indispensable for the mitochondrial translocation and the substrate degradation (Supplementary Fig. S8). Interestingly, Parkin mutant lacking the Ubl domain (ΔUbl) showed a mild delay in the mitochondrial translocation, slowed the mitochondrial reorganization to the perinuclear region (Supplementary Fig. S8b and c) and impaired the degradation of mitochondrial outer membrane proteins (Supplementary Fig. S8d). These results suggest that proper regulation of the Parkin Ubl domain through the Ser65 phosphorylation is required not only for efficient translocation to mitochondria as an initial step of mitophagy, but also for the degradation of mitochondrial outer membrane proteins during mitophagy through an as yet unknown mechanism.

Discussion

A series of *Drosophila* genetic and cell biological studies have clearly demonstrated that PINK1 is required for Parkin-mediated mitochondrial maintenance. The mitophagy of damaged mitochondria is a well-characterised event in which PINK1 and Parkin are involved. However, how PINK1 regulates Parkin is largely unclear. This study has shown that Ser65 in the Ubl domain of endogenous Parkin is phosphorylated in an activated PINK1-dependent manner. In addition to mitochondrial accumulation of PINK1, ΔΨm depolarisation-dependent PINK1 autophosphorylation has been reported to be an important element for PINK1 activation and Parkin recruitment[19,29]. Consistent with these observations, our investigation of PINK1 siRNA suggests that a lower level of PINK1 is able to phosphorylate Parkin after ΔΨm depolarisation (Fig. 1c, compare lanes 1 and 4). Our domain analysis of PINK1 demonstrates that intact PINK1 is required for CCCP-dependent Parkin phosphorylation, and the lack of phosphorylation in fibroblasts from a *PARK6* patient implies relevance to the pathogenesis of PD.

The biological significance of this phosphorylation event is suggested by the fact that replacement of Ser65 with alanine or glutamic acid impairs the mitochondrial translocation of Parkin and/or the subsequent mitophagy process. Our observation that maximal phosphorylation of Parkin occurs within 1 hr of CCCP treatment supports the idea that Ser65 phosphorylation is required for the early step of Parkin translocation. In contrast, PINK1 accumulation appears to last at least 6 hr (Fig. 4c and Supplementary Fig. S1b). The difference in time course between PINK1 accumulation and Parkin phosphorylation could be explained by the observation that phosphorylated Parkin is degraded by proteasomal activity. The biochemical evidence that only the phosphorylated form of endogenous Parkin is present in the mitochondrial fraction also implies that Parkin phosphorylation is an essential event for its mitochondrial translocation and subsequent activation (Fig. 3c and Supplementary Fig. S6). Overexpression of PINK1 and Parkin itself leads to mitochondrial translocation of Parkin independently of ΔΨm depolarization, which suggests that excessive amounts of PINK1 and Parkin do not faithfully reflect endogenous reactions. Our study using *PINK1*$^{-/-}$ MEFs stably co-expressing PINK1 and GFP-Parkin might also be saddled with such a problem. We believe that the endogenous observation in which phosphorylated Parkin is accumulated in mitochondria is a more reliable proposal as a molecular model. The delay of exogenous GFP-Parkin S65A in the mitochondrial translocation would indicate that modification of Ser65 is important for Parkin translocation at least. At the same time, another important finding is that pathogenic mutants that lose their translocation activity are also phosphorylated (Fig. 3b), raising the possibility that phosphorylation of Parkin at Ser65 is insufficient for translocation. Thus, Ser65 phosphorylation likely leads to other events in mitochondrial translocation, such as the association or dissociation of protein(s) involved in the mitochondrial translocation of Parkin or the modification of Parkin itself for activation at a different site(s).

Both the S65A and S65E Parkin mutants cannot undergo efficient mitophagy, as indicated by the incomplete degradation of

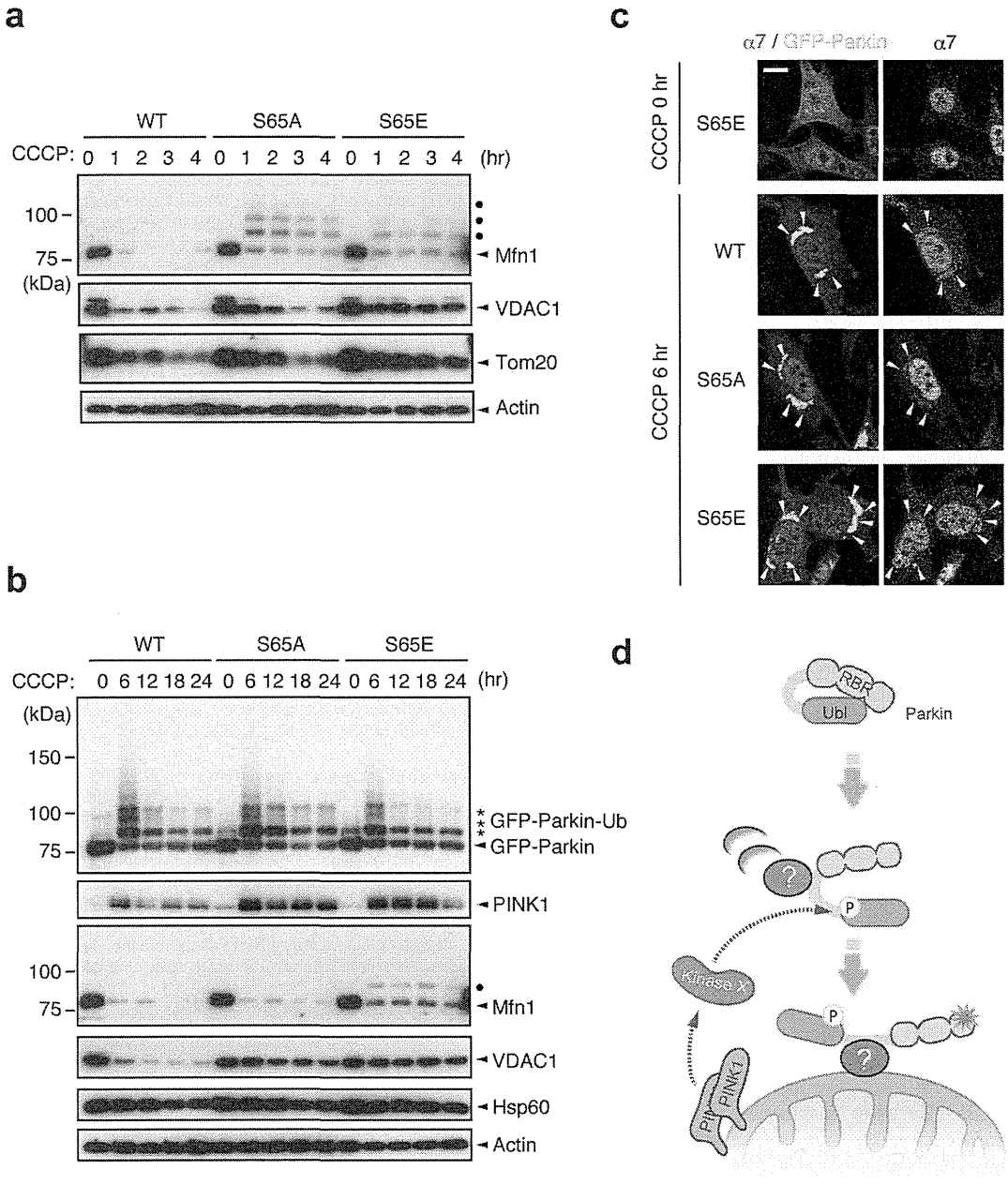

Figure 4 | Ser65 phosphorylation affects the subsequent autophagy reaction. (a) CCCP-dependent degradation of mitochondrial outer membrane proteins in PINK1 WT/*PINK1*$^{-/-}$ MEFs expressing WT or mutant forms of GFP-Parkin. Mfn1, VDAC1 and Tom20 were used as markers of mitochondrial outer membrane proteins. Actin: a loading control. Dots: ubiquitinated Mfn1. (b) Long-term time-course analysis of CCCP-dependent mitochondrial protein degradation. The degradation of outer membrane proteins was impaired in cells expressing GFP-Parkin S65A or S65E mutations. Hsp60 was used as a marker of mitochondrial matrix proteins. (c) S65A and S65E mutations do not affect proteasome recruitment to the mitochondria during mitophagy. PINK1 WT/*PINK1*$^{-/-}$ MEFs expressing WT or mutant forms of GFP-Parkin (green) were treated with 30 μM CCCP for 3 or 6 hr. Cells were stained with anti-proteasome subunit alpha type 7 (α7, red). α7-immunoreactivity was enriched in the nuclei of all three cell genotypes under normal conditions, as displayed in the representative image of S65E (CCCP 0 hr), and overlapped with the aggregated mitochondria (arrowheads) 6 hr after CCCP treatment irrespective of genotype. Similar results were obtained 3 hr after CCCP treatment. Scale bar = 10 μm. (d) Model for Parkin translocation and activation. The Parkin Ubl domain masks C-terminal RING-IBR-RING (RBR) domains for E3 activity[46]. A Parkin phosphorylation event at Ser65 (P), combined with unknown factor(s) (?), stimulates the mitochondrial translocation of Parkin, releasing the RBR domains from autoinhibition by the Ubl domain.

the mitochondrial outer membrane proteins. Because inhibition of the degradation of the mitochondrial outer membrane proteins by proteasome inhibitors is reported to block mitophagy[32,35], it may be that the modification of Parkin Ser65 has a greater than expected impact on the mitophagy process. Although our study does not demonstrate that the S65E mutant behaves exactly like the phosphorylated form of Parkin, the S65E mutant does translocate to the mitochondria in a similar way to WT, although with slightly impaired efficiency, suggesting that S65E has at least some properties that are similar to phosphorylated Parkin. Currently, it is unknown why S65E also inhibits the later processes of mitophagy. One possible explanation is that rapid degradation of phosphorylated Parkin is required for the proper progression of mitophagy, and S65E may not be degraded effectively. However,

there is no evidence that S65E is more stable than WT, as shown in Figure 4c.

Very recently, Kondapalli *et al.* proposed a model to explain the biological significance of Ser65 phosphorylation, in which Ser65 phosphorylation relieves autoinhibition of Parkin E3 activity by the Ubl domain[18]. This model may explain the depolarised $\Delta\Psi$m-dependent activation of Parkin. However, our data indicated that the Parkin S65A mutant is also autoubiquitinated (Fig. 4b) and that the ΔUbl mutant showed mild translocation defect and impaired substrate degradation (Supplementary Fig. S8). Moreover, if this is the case, the E3 activity of Parkin pathogenic mutants lacking mitochondrial translocational activity but harbouring intact E3 activity *in vitro* (such as K161N and K211N, which are subjected to the Ser65 phosphorylation) should be activated in the cytosol[38]. However, our previous data indicate that K161N and K211N are not activated by CCCP treatment[23]. Thus, it is conceivable that another step is required for depolarised $\Delta\Psi$m-dependent activation of Parkin E3. In addition, the Ubl domain might not only autoinhibit its E3 activity but also contribute to the mitochondrial translocation and the substrate degradation through an as yet unknown mechanism. We believe that an appropriate way to estimate Parkin E3 activity in the context of mitophagy is to evaluate the ubiquitination and degradation of substrates in cells with depolarised $\Delta\Psi$m. Mfn1 is a well-characterised direct substrate of Parkin[32], and Parkin-dependent poly-ubiquitination modification of Mfn1 can be detected by Western blotting upon $\Delta\Psi$m depolarisation[32,39,40]. Parkin S65A and S65E appear to ubiquitinate Mfn1, as poly-ubiquitinated forms of Mfn1 were observed (Fig. 4b). However, they cannot degrade it effectively, which suggests that the process of substrate degradation is also impaired in these mutants.

Kondapalli *et al.* have also shown that *T. castaneum* PINK1 (TcPINK1) directly phosphorylates human Parkin at Ser65[18]. We confirmed their finding using recombinant TcPINK1 produced from the same construct (Supplementary Fig. S4). The replacement of MBP-Parkin Ser65 with alanine completely abolished PINK1-mediated phosphorylation, indicating that Ser65 is the sole phosphorylation site *in vitro*. However, experiments in cultured cells showed that the replacement of Ser9, Ser10, Ser101 and Ser198 with alanine affects the Ser65 phosphorylation efficiency (Ser9, ~35% reduction; Ser10, ~76% reduction; Ser101, ~65% reduction; Ser198, ~92% reduction) (Fig. 2a). These residues might be priming phosphorylation sites for Ser65 phosphorylation.

Because PINK1 is believed to be activated in the mitochondria, a topological inconsistency arises from our cell-based data that cytosolic Parkin lacking the mitochondrial translocation activity is phosphorylated. Therefore, it is possible that PINK1 indirectly regulates Parkin phosphorylation. One possible explanation for this is the presence of another cytosolic kinase(s) regulated by PINK1 (Fig. 4d). Alternatively, because mitochondria are a dynamic organelle, cytosolic Parkin adjacent to the moving and fragmented mitochondria with depolarised $\Delta\Psi$m might be phosphorylated incidentally. The issue as to whether or not PINK1 directly phosphorylates Parkin in cells remains to be solved.

In conclusion, this study has suggested that PINK1-dependent Parkin phosphorylation at Ser65 accelerates the mitochondrial translocation of Parkin and showed that the introduction of mutations at this site also affects subsequent mitophagy processes. Concurrently, our data provide the possibility that there is an elaborate multi-step mechanism for the mitochondrial translocation of Parkin upon the loss of $\Delta\Psi$m (Fig. 4d), the clarification of which awaits further study.

Methods

Antibodies, plasmids and cell lines. Antibodies used in Western blot analysis were as follows: anti-Parkin (1 : 1,000 and 1 : 5,000 dilution for endogenous and exogenous Parkin, respectively; Cell Signaling Technology, clone PRK8), anti-PINK1 (1 : 1,000 dilution; Novus, BC100-494 or 1 : 1,000 dilution; Cell Signaling Technology, clone D8G3), anti-Mfn1 (1 : 1,000 dilution; Abnova, clone 3C9), anti-VDAC1 (1 : 1,000 dilution; Abcam, Ab15895), anti-Tom20 (1 : 500 dilution; Santa Cruz Biotechnology, FL-145), anti-FLAG-HRP (1 : 2,000 dilution; Sigma-Aldrich, clone M2), anti-GFP (1 : 5,000 dilution; Abcam, ab290), anti-Actin (1 : 10,000 dilution; Millipore, MAb1501), anti-LDH (1 : 1,000 dilution; Abcam, ab7639-1), anti-phospho-GSK3ß (1 : 1,000 dilution; Cell Signaling Technology, clone 5B3), anti-GSK3ß (1 : 1,000 dilution; Cell Signaling Technology, clone 27C10), and anti-Hsp60 (1 : 10,000 dilution; BD Biosciences, clone 24/Hsp60). Antibodies used in immunocytochemistry were as follows: FITC-conjugated anti-GFP (1 : 1,000 dilution; Abcam, ab6662), anti-Tom20 (1 : 1,000 dilution; Santa Cruz Biotechnology, FL-145), anti-Myc (1 : 500 dilution; Millipore, clone 4A6), anti-p62 (1: 500 dilution; Progen Biotechnik, GP62-C), anti-Parkin (1 : 1,000 dilution; Cell Signaling Technology, clone PRK8) and anti-proteasome α7 (1 : 250; a kind gift of Dr S. Murata at the University of Tokyo). cDNAs for human Parkin, PINK1 and its pathogenic and engineered mutants are as described in previous studies[23,41]. Parkin phospho-mutants were generated by PCR-based mutagenesis followed by sequencing confirmation of the entire gene. *PINK1*$^{-/-}$ MEFs, cultured as previously described[23], were retrovirally transfected with pMXs-puro harbouring non-tagged PINK1, PINK1-FLAG, non-tagged Parkin, HA-Parkin, GFP-Parkin and related cDNA; transfected cells were then selected with 1 μg/ml puromycin. HeLa cells maintained at 37°C in a 5% CO_2 atmosphere in Dulbecco's Modified Eagle's Medium (DMEM) supplemented with 10% FCS and 1x non-essential amino acids (GIBCO) were retrovirally transfected with pMXs-puro harbouring non-tagged Parkin along with pcDNA3Hyg-mSlc7a1-VSVG and pcDNA3Hyg-mSlc7a1-FLAG (a kind gift of Dr N. Fujita at UCSD). Stable cell lines were selected with 1 μg/ml puromycin and cloned. Transient transfections of cultured cells were performed using Lipofectamine 2000 (Invitrogen) for plasmids and Lipofectamine RNAiMAX (Invitrogen) for stealth siRNA duplexes (Invitrogen), which were used according to the manufacturer's instructions.

Tissue culture. Skin biopsies were obtained from a *PARK6* case and a control without mutations in any known PD genes. The study was approved by the ethics committee of Juntendo University, and all participants gave written, informed consent. Dermal primary fibroblasts established from biopsies were cultured in high glucose DMEM supplemented with 10% foetal bovine serum, 1x non-essential amino acids, 1 mM sodium pyruvate (GIBCO), 100 μM 2-mercaptoethanol, and 1% penicillin–streptomycin at 37°C in a 5% CO_2 atmosphere.

Mapping of Parkin phosphorylation sites. *PINK1*$^{-/-}$ MEFs (6.0 x 10^7) expressing HA-Parkin and PINK1-FLAG were treated with or without 30 μM CCCP for 30 min. HA-Parkin (~500 ng in each) immunopurified with anti-HA-conjugated agarose beads was eluted with 8 M urea buffered with 50 mM Tris-HCl at pH 9.0. Samples from two independent experiments were digested with trypsin or chymotrypsin and analysed by nano-scale liquid chromatography-tandem mass spectrometry (Dionex Ultimate3000 RSLCnano and ABSciex TripleTOF 5600) followed by MASCOT searching and Mass Navigator/PhosPepAnalyzer processing for identification and label-free quantitation, respectively[42]. Determination of phosphosite localisation was performed based on the presence of site-determining ions[43].

Phosphorylation assay and mitochondrial fractionation. *PINK1*$^{-/-}$ MEFs harbouring HA-Parkin along with wild-type or a kinase-dead form of PINK1-FLAG were metabolically labelled with 175 μCi/ml of [^{32}P] orthophosphate in phosphate-free DMEM (GIBCO) with 10% FBS at 37°C for 3 hr. The medium was then replaced with fresh DMEM containing 10% FBS. Cells were treated with CCCP for 1.5 hr and were lysed on ice with lysis buffer containing 0.2% NP-40, 50 mM Tris (pH 7.4), 150 mM NaCl and 10% glycerol supplemented with protease inhibitor (Roche Diagnostics) and phosphatase inhibitor (Pierce) cocktails, and HA-Parkin and PINK1-FLAG were immunoprecipitated with anti-HA (Wako Pure Chemical, clone 4B2)- or anti-FLAG (Sigma-Aldrich, clone M2)-conjugated agarose beads. Immunoprecipitates were separated by SDS-PAGE and transferred onto a PVDF membrane. Autoradiography and Western blotting were performed to visualise proteins. Phos-tag Western blotting was performed as previously described[28]. Briefly, phospho-Parkin and phospho-PINK1 were separated on 8% gels containing 50 μM Phos-tag. Mitochondrial and cytosolic fractionations were performed as previously described, with some modifications[20]. The cytosolic fractions were further clarified by a second centrifugation at 105,000 *g* for 60 min to remove residual organelle membranes.

Immunocytochemical analysis. Cells plated on 3.5 mm glass-bottom dishes (MatTek) were fixed with 4% paraformaldehyde in PBS and permeabilised with 50 μg/ml digitonin for anti-Tom20 and anti-p62 staining or with 0.1% NP-40 for anti-α7 staining in PBS. Cells were stained with anti-Tom20 or anti-α7 antibodies in combination with FITC-conjugated anti-GFP antibody and were counterstained with DAPI for nuclei. Cells were imaged using laser-scanning microscope systems (TCS-SP5, Leica or LSM510 META, Carl Zeiss).

Statistical analysis. A one-way repeated measures ANOVA was used to determine significant differences between multiple groups unless otherwise indicated. If a significant result was achieved ($p < 0.05$), the means of the control and the specific test group were analysed using the Tukey-Kramer test.

1. Valente, E. M. *et al.* Hereditary early-onset Parkinson's disease caused by mutations in PINK1. *Science* **304**, 1158–1160 (2004).

2. Takatori, S., Ito, G. & Iwatsubo, T. Cytoplasmic localization and proteasomal degradation of N-terminally cleaved form of PINK1. *Neurosci Lett* **430**, 13–17 (2008).
3. Beilina, A. *et al.* Mutations in PTEN-induced putative kinase 1 associated with recessive parkinsonism have differential effects on protein stability. *Proc Natl Acad Sci U S A* **102**, 5703–5708 (2005).
4. Silvestri, L. *et al.* Mitochondrial import and enzymatic activity of PINK1 mutants associated to recessive parkinsonism. *Hum Mol Genet* **14**, 3477–3492 (2005).
5. Sim, C. H. *et al.* C-terminal truncation and Parkinson's disease-associated mutations down-regulate the protein serine/threonine kinase activity of PTEN-induced kinase-1. *Hum Mol Genet* **15**, 3251–3262 (2006).
6. Clark, I. E. *et al.* Drosophila pink1 is required for mitochondrial function and interacts genetically with parkin. *Nature* **441**, 1162–1166 (2006).
7. Park, J. *et al.* Mitochondrial dysfunction in Drosophila PINK1 mutants is complemented by parkin. *Nature* **441**, 1157–1161 (2006).
8. Yang, Y. *et al.* Mitochondrial pathology and muscle and dopaminergic neuron degeneration caused by inactivation of Drosophila Pink1 is rescued by Parkin. *Proc Natl Acad Sci U S A* **103**, 10793–10798 (2006).
9. Kitada, T. *et al.* Mutations in the parkin gene cause autosomal recessive juvenile parkinsonism. *Nature* **392**, 605–608 (1998).
10. Imai, Y., Soda, M. & Takahashi, R. Parkin suppresses unfolded protein stress-induced cell death through its E3 ubiquitin-protein ligase activity. *J Biol Chem* **275**, 35661–35664 (2000).
11. Shimura, H. *et al.* Familial Parkinson disease gene product, parkin, is a ubiquitin-protein ligase. *Nat Genet* **25**, 302–305 (2000).
12. Zhang, Y. *et al.* Parkin functions as an E2-dependent ubiquitin- protein ligase and promotes the degradation of the synaptic vesicle-associated protein, CDCrel-1. *Proc Natl Acad Sci U S A* **97**, 13354–13359 (2000).
13. Deas, E. *et al.* PINK1 cleavage at position A103 by the mitochondrial protease PARL. *Hum Mol Genet* **20**, 867–879 (2011).
14. Jin, S. M. *et al.* Mitochondrial membrane potential regulates PINK1 import and proteolytic destabilization by PARL. *J Cell Biol* **191**, 933–942 (2010).
15. Meissner, C., Lorenz, H., Weihofen, A., Selkoe, D. J. & Lemberg, M. K. The mitochondrial intramembrane protease PARL cleaves human Pink1 to regulate Pink1 trafficking. *J Neurochem* **117**, 856–867 (2011).
16. Whitworth, A. J. *et al.* Rhomboid-7 and HtrA2/Omi act in a common pathway with the Parkinson's disease factors Pink1 and Parkin. *Dis Model Mech* **1**, 168–174; discussion 173 (2008).
17. Narendra, D. P. *et al.* PINK1 is selectively stabilized on impaired mitochondria to activate Parkin. *PLoS Biol* **8**, e1000298 (2010).
18. Kondapalli, C. *et al.* PINK1 is activated by mitochondrial membrane potential depolarization and stimulates Parkin E3 ligase activity by phosphorylating Serine 65. *Open Biol* **2**, 120080 (2012).
19. Okatsu, K. *et al.* PINK1 autophosphorylation upon membrane potential dissipation is essential for Parkin recruitment to damaged mitochondria. *Nat Commun* **3**, 1016 (2012).
20. Lazarou, M., Jin, S. M., Kane, L. A. & Youle, R. J. Role of PINK1 binding to the TOM complex and alternate intracellular membranes in recruitment and activation of the E3 ligase Parkin. *Dev Cell* **22**, 320–333 (2012).
21. Vives-Bauza, C. *et al.* PINK1-dependent recruitment of Parkin to mitochondria in mitophagy. *Proc Natl Acad Sci U S A* **107**, 378–383 (2010).
22. Geisler, S. *et al.* PINK1/Parkin-mediated mitophagy is dependent on VDAC1 and p62/SQSTM1. *Nat Cell Biol* **12**, 119–131 (2010).
23. Matsuda, N. *et al.* PINK1 stabilized by mitochondrial depolarization recruits Parkin to damaged mitochondria and activates latent Parkin for mitophagy. *J Cell Biol* **189**, 211–221 (2010).
24. Kawajiri, S. *et al.* PINK1 is recruited to mitochondria with parkin and associates with LC3 in mitophagy. *FEBS Lett* **584**, 1073–1079 (2010).
25. Ziviani, E., Tao, R. N. & Whitworth, A. J. Drosophila parkin requires PINK1 for mitochondrial translocation and ubiquitinates mitofusin. *Proc Natl Acad Sci U S A* **107**, 5018–5023 (2010).
26. Sha, D., Chin, L. S. & Li, L. Phosphorylation of parkin by Parkinson disease-linked kinase PINK1 activates parkin E3 ligase function and NF-kappaB signaling. *Hum Mol Genet* **19**, 352–363 (2010).
27. Kim, Y. *et al.* PINK1 controls mitochondrial localization of Parkin through direct phosphorylation. *Biochem Biophys Res Commun* **377**, 975–980 (2008).
28. Imai, Y. *et al.* The loss of PGAM5 suppresses the mitochondrial degeneration caused by inactivation of PINK1 in Drosophila. *PLoS Genet* **6**, e1001229 (2010).
29. Woodroof, H. I. *et al.* Discovery of catalytically active orthologues of the Parkinson's disease kinase PINK1: analysis of substrate specificity and impact of mutations. *Open Biol* **1**, 110012 (2011).
30. Yamamoto, A. *et al.* Parkin phosphorylation and modulation of its E3 ubiquitin ligase activity. *J Biol Chem* **280**, 3390–3399 (2005).
31. Narendra, D., Tanaka, A., Suen, D. F. & Youle, R. J. Parkin is recruited selectively to impaired mitochondria and promotes their autophagy. *J Cell Biol* **183**, 795–803 (2008).
32. Tanaka, A. *et al.* Proteasome and p97 mediate mitophagy and degradation of mitofusins induced by Parkin. *J Cell Biol* **191**, 1367–1380 (2010).
33. Okatsu, K. *et al.* p62/SQSTM1 cooperates with Parkin for perinuclear clustering of depolarized mitochondria. *Genes Cells* **15**, 887–900 (2010).
34. Narendra, D., Kane, L. A., Hauser, D. N., Fearnley, I. M. & Youle, R. J. p62/SQSTM1 is required for Parkin-induced mitochondrial clustering but not mitophagy; VDAC1 is dispensable for both. *Autophagy* **6**, 1090–1106 (2010).
35. Chan, N. C. *et al.* Broad activation of the ubiquitin-proteasome system by Parkin is critical for mitophagy. *Hum Mol Genet* **20**, 1726–1737 (2011).
36. Wang, X. *et al.* PINK1 and Parkin Target Miro for Phosphorylation and Degradation to Arrest Mitochondrial Motility. *Cell* **147**, 893–906 (2011).
37. Liu, S. *et al.* Parkinson's disease-associated kinase PINK1 regulates Miro protein level and axonal transport of mitochondria. *PLoS Genet* **8**, e1002537 (2012).
38. Matsuda, N. *et al.* Diverse effects of pathogenic mutations of Parkin that catalyze multiple monoubiquitylation in vitro. *J Biol Chem* **281**, 3204–3209 (2006).
39. Gegg, M. E. *et al.* Mitofusin 1 and mitofusin 2 are ubiquitinated in a PINK1/parkin-dependent manner upon induction of mitophagy. *Hum Mol Genet* **19**, 4861–4870 (2010).
40. Rakovic, A. *et al.* Mutations in PINK1 and Parkin impair ubiquitination of Mitofusins in human fibroblasts. *PLoS One* **6**, e16746 (2011).
41. Shiba, K. *et al.* Parkin stabilizes PINK1 through direct interaction. *Biochem Biophys Res Commun* **383**, 331–335 (2009).
42. Iwasaki, M., Sugiyama, N., Tanaka, N. & Ishihama, Y. Human proteome analysis by using reversed phase monolithic silica capillary columns with enhanced sensitivity. *J Chromatogr A* **1228**, 292–297 (2012).
43. Beausoleil, S. A., Villen, J., Gerber, S. A., Rush, J. & Gygi, S. P. A probability-based approach for high-throughput protein phosphorylation analysis and site localization. *Nat Biotechnol* **24**, 1285–1292 (2006).
44. Li, Y. *et al.* Clinicogenetic study of PINK1 mutations in autosomal recessive early-onset parkinsonism. *Neurology* **64**, 1955–1957 (2005).
45. Zhou, C. *et al.* The kinase domain of mitochondrial PINK1 faces the cytoplasm. *Proc Natl Acad Sci U S A* **105**, 12022–12027 (2008).
46. Chaugule, V. K. *et al.* Autoregulation of Parkin activity through its ubiquitin-like domain. *EMBO J* **30**, 2853–2867 (2011).

Acknowledgements

We thank: Drs K. Tanaka, N. Matsuda, K. Okatsu, T. Kitamura, S. Murata, N. Fujita, N. Furuya, M.M.K. Muqit and R.J. Youle for their generous supply of materials; T. Hasegawa and Y. Imaizumi for the preparation of human fibroblasts; and T. Imura for her technical help. This study was supported by the Naito Foundation, the Novartis Foundation, the Grant-in-Aid for Young Scientists (B) from MEXT in Japan (SK-F, YI), the CREST program of JST (NH) and Grant-in-Aid for Scientific Research on Innovative Areas (NH).

Author contributions

K.S., Y. Imai and N.H. designed the research; K.S., Y. Imai, S.Y., T.K. and Y. Ishihama performed the experiments; S.S. contributed new reagents/analytic tools; K.S. and Y. Imai analysed the data; and Y. Imai and N.H. wrote the paper. K.S. and Y. Imai contributed equally to this work.

Additional information

Supplementary information accompanies this paper at http://www.nature.com/scientificreports

Competing financial interests: The authors declare no competing financial interests.

How to cite this article: Shiba-Fukushima, K. *et al.* PINK1-mediated phosphorylation of the Parkin ubiquitin-like domain primes mitochondrial translocation of Parkin and regulates mitophagy. *Sci. Rep.* 2, 1002; DOI:10.1038/srep01002 (2012).

BRIEF REPORT

Pseudo-heterozygous Rearrangement Mutation of *parkin*

Manabu Funayama, PhD,[1,2*] Hiroyo Yoshino, PhD,[1] Yuanzhe Li, MD, PhD,[1] Hiromichi Kusaka, DB,[2] Hiroyuki Tomiyama, MD, PhD,[2,3] and Nobutaka Hattori, MD, PhD[1,2,3*]

[1]*Research Institute for Diseases of Old Age, Graduate School of Medicine, Juntendo University, Tokyo, Japan;* [2]*Department of Neurology, Juntendo University School of Medicine, Tokyo, Japan;* [3]*Department of Neuroscience for Neurodegenerative Disorders, Juntendo University School of Medicine, Tokyo, Japan*

ABSTRACT

Background: Mutations in *parkin* are the most frequent cause of autosomal recessive parkinsonism. Quantitative PCR is used to detect *parkin* rearrangements. However, the method has an inherent problem—deletion and duplication in the same allelic exon could be determined as normal. To present this misidentification, we report a family with compound heterozygous rearrangements in *parkin*. **Methods:** A patient with early-onset parkinsonism and the parents were investigated by quantitative PCR, haplotype analysis, reverse-transcription PCR, and direct sequencing. **Results:** A single heterozygous duplication (duplication of exons 6–7) was identified in the patient by quantitative PCR. Detailed analysis of the family revealed the patient carried compound heterozygous of combined deletion (deletion of exons 3–5) and duplication (duplication of exons 3–7). **Conclusions:** For correct determination of rearrangement mutation, mutation analysis of the patient as well as other family members and/or break-point analysis of genomic DNA and at the transcript level should be conducted.

Key Words: Parkinson's disease; rearrangement; parkin; compound heterozygote; gene dosage

Parkinson's disease (PD) is the most common progressive neurological movement disorder involving loss of neurons in the substantia nigra. Although most patients have sporadic PD, 5%–10% of patients have a positive family history of PD. Mutations in *parkin* (MIM 602544; *PARK2*) are the most common cause of autosomal recessive early-onset parkinsonism.[1,2] So far, various mutations of *parkin* have been identified including rearrangements (deletions and multiplications) and point mutations.[3–5] In addition, there is controversy about whether a single heterozygous mutation of *parkin* also associates with familial as well as sporadic PD.[6,7] Thus, screening for *parkin* mutations is important to elucidate the pathogenesis of not only *parkin*-linked parkinsonism but also of sporadic PD.

In general, homozygous exonic deletion and point mutations are screened by polymerase chain reaction (PCR) and direct sequencing.[1] Multiplication and single heterozygous exonic deletions are analyzed by quantitative PCR (qPCR).[8] However, there is a limitation in the method of qPCR because exonic rearrangement can be misidentified. For example, compound heterozygous mutations for deletion and duplication in the same allelic exons can be determined as normal.

In the present study, to demonstrate the problem of screening for exonic rearrangement, we applied detailed genetic analysis to investigate *parkin* mutations in a Japanese family with early-onset parkinsonism.

Subjects and Methods

Subjects

This study was approved by the ethics committee of Juntendo University School of Medicine. Each subject provided informed consent. One patient with early-onset parkinsonism and her parents were investigated for *parkin* mutations. Array comparative genomic hybridization analysis confirmed the break point of *PARK2*, as described previously.[9] The index patient was a 21-year-old Japanese woman. She initially showed akinesia with gait disturbance in the right lower limb at age 15. Two years later, the patient developed resting tremor in the upper limb and right

Additional Supporting Information may be found in the online version of this article.

***Correspondence to:** Drs. Manabu Funayama or Nobutaka Hattori, Research Institute for Diseases of Old Age, Graduate School of Medicine, Juntendo University, 2-1-1 Hongo, Bunkyo-ku, Tokyo 113-8421, Japan; funayama@juntendo.ac.jp

Funding agencies: This work was supported by the Strategic Research Foundation Grant-in-Aid Project for Private Universities, Grants-in-Aid for Scientific Research (to N.H., 80218510, and to H.T., 21591098), Grant-in-Aid for Young Scientists (to M.F., 22790829, and to Y.L., 23791003), Grant-in-Aid for Scientific Research on Innovative Areas (to M.F. 23129506) from the Japanese Ministry of Education, Culture, Sports, Science and Technology, and Project Research Grants-in-Aid (to M.F., 1041 and 2334) from Juntendo University School of Medicine.

Relevant conflicts of interest/financial disclosures: Nothing to report. Full financial disclosures and author roles may be found in the online version of this article.

Received: 4 July 2011; **Revised:** 11 November 2011; **Accepted:** 12 December 2011

Published online in Wiley Online Library (wileyonlinelibrary.com). DOI: 10.1002/mds.24906

lower limb (Hoehn and Yahr stage I). She had a good response to levodopa treatment but developed levodopa-induced dyskinesias during treatment. The parents were nonconsanguineous and free of PD or any other neurodegenerative disease.

Genetic Analysis of *parkin*

Genomic DNA was isolated from peripheral blood using a QIAamp blood Maxi Kit (Qiagen, Valencia, CA). All exons of *parkin* were amplified by PCR. PCR amplicons were separated and visualized by 2% agarose gel electrophoresis. After purification of PCR amplicons using ExoSAP IT (GE Healthcare, Salt Lake City, UT), direct sequencing was carried out by a Big Dye Terminator v1.1 Cycle Sequencing Kit (Applied Biosystems, Foster City, CA) and a 3130 Genetic Analyzer (Applied Biosystems, Foster City, CA). The gene dosage of *parkin* was analyzed by qPCR using TaqMan Fast Universal Master Mix (Applied Biosystems, Foster City, CA) and a 7500 Fast Real-Time PCR system (Applied Biosystems, Foster City, CA).

Semiquantitative haplotype analysis was performed by PCR using fluorescent-labeled primers and 3130 Genetic Analyzer (Applied Biosystems, Foster City, CA). We genotyped 12 microsatellites on the *PARK2* locus including D6S1723, D6S1277, D6S1599, D6S980, D6S955, D6S305, D6S411, AFMa155td9, AFMb281wf1, D6S1579, D6S1035, and D6S2436. The sequences of the primers and the conditions of PCR have been described previously.[1,8] Total RNA was isolated from peripheral blood using a PAXgene Blood RNA Kit (Qiagen, Valencia, CA). Total RNA (500 ng) was used to synthesize cDNA using a TaKaRa RNA PCR Kit (AMV) version 3.0 (Takara Bio, Shiga, Japan) and random 9-mer primer (Takara Bio, Shiga, Japan). The cDNA was amplified by PCR using KOD-FX (TOYOBO, Osaka, Japan), and the following primers: 5′-GTTCCGGCTGACCAGTTGC-3′ and 5′-CCGGTTGTACTGCTCTTCTCCC3′, for detection of deletion; 5′-CCAGTGACCATGATAGTGTT-3′ and 5′-TGAAGGTAGACACTGGGTAT-3′, for detection of multiplication.[10] Reverse-transcriptase PCR (RT-PCR) products were separated and visualized by 2% agarose gel electrophoresis. Subsequently, each of the bands was cut out and eluted using a QIAquick Gel Extraction Kit (Qiagen, Valencia, CA). Purified RT-PCR products were sequenced using a Big Dye Terminator v1.1 Cycle Sequencing Kit (Applied Biosystems, Foster City, CA).

Results

None of the point mutations of *parkin* or homozygous exonic deletions were detected in any of the 3 family members. Heterozygous duplications of exons 6 and 7 (EX6–7 dup) of *parkin* were detected in the patient with parkinsonism by gene dosage analysis using qPCR (Fig. 1). However, the parents did not have the same mutation as the patient. Instead, heterozygous duplications from exons 3–7 (EX3–7 dup) were detected in the father, and heterozygous deletions from exons 3–5 (EX3–5 del) were detected in the mother (Fig. 1).

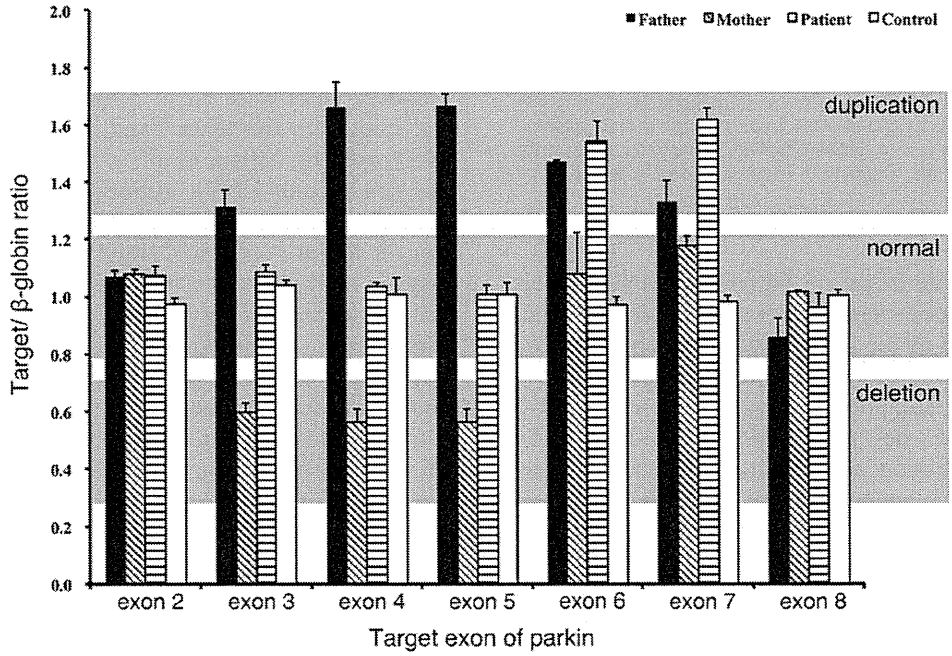

FIG. 1. Gene-dosage analysis of *parkin* using qPCR. Gene dosage of *parkin* was normalized to the dosage of β-*globin*. Values between 0.3 and 0.7 represent heterozygous deletion, between 0.8 and 1.2 are normal, and between 1.3 and 1.7 represent heterozygous duplication. Data are means ± SEMs.

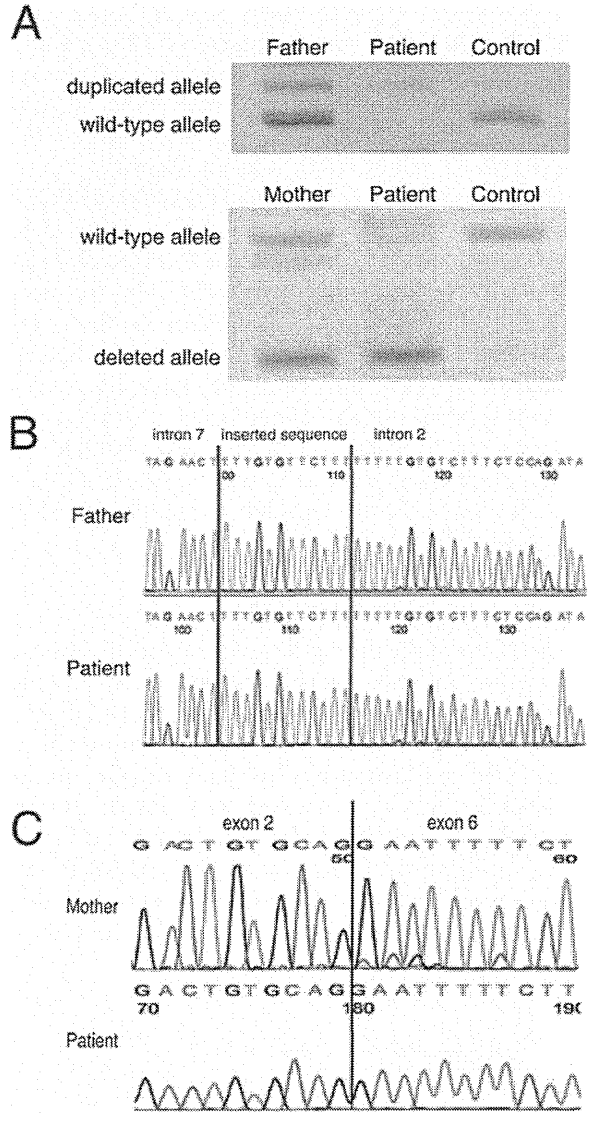

FIG. 2. RT-PCR analysis (**A**) and break-point analysis (**B, C**) of *parkin*. A duplicated allele and a deleted allele were detected in the patient. A break point from introns 7 to 2 was observed in genomic DNA of the patient and the father (**B**). Skipping of exons 3–5 was observed in the *parkin* transcript (**C**).

To determine the mutation pattern of *parkin* in this family, we performed semiquantitative haplotype analysis. Comparison of the peak height of each allele and genotyping results showed a pattern compatible with the patient being compound heterozygous with EX3–7 dup and EX3–5 del (Supporting Fig. 1A,B). To confirm this prediction of the mutation pattern of *parkin* in our patient, we carried out RT-PCR and direct sequencing. The results showed that 2 of the abnormal alleles (EX 3–7dup and EX3–5 del) were inherited from the parents (Fig. 2A–C). Furthermore, the parents harbored a single heterozygous exonic rearrangement of *parkin*. We detected a sequence of the duplicated break point in the patient and the father, and exon skipping of *parkin* was observed at the transcript level in the patient and the mother (Fig. 2A–C). Because recurrent tandem duplication of introns 2–7 of *parkin* have been reported,[9] only 1 break point was observed in the patient and the father (Fig. 2B).

Discussion

Mutations of *parkin* are the most frequent cause of autosomal recessive early-onset parkinsonism, and thus unaffected carriers with single heterozygous *parkin* mutation are thought to exist. In this study, we demonstrated the incorrect determination of *parkin* rearrangement mutation using qPCR assay based on the combination of duplication and deletion in the same allelic exons. This erroneous decision is difficult to avoid by examining gene dosage in only patients with parkinsonism.

Recently, single heterozygous mutations of genes such as *parkin* and *PINK1* associated with autosomal recessive familial parkinsonism were considered risk and modifying factors for sporadic PD as well as familial PD.[6,7,11–13] If a single heterozygous rearrangement in contiguous exons is found by qPCR, it cannot be determined if this rearrangement exists on the same allele. *Parkin* exists in a common fragile site, and exonic rearrangements of *parkin* are frequently reported in patients with parkinsonism from various racial and ethnic groups.[1–5,9] Therefore, it is important to be precise when determining the mutation pattern.

Various methods are currently employed for detection of copy-number variations (CNVs), such as qPCR, multiplex ligation-dependent probe amplification (MLPA), and microarray-based CNV assay.[14] qPCR and MLPA are convenient and rapid methods that use small aliquots of genomic DNA to analyze CNV-mapped limited loci. However, these methods could produce false CNV results, as seen in the present study. On the other hand, the high-density microarray used by Mitsui et al[9] is suitable for determining the structure of CNVs, although it is not designed for routine screening of CNVs. Reflecting on such a situation, it is our view that subjects with a single heterozygous rearrangement mutation of *parkin* should at least be examined by RT-PCR analysis. Although the examination cannot detect the mutation with 100% sensitivity, the observation of transcript formation could be helpful in determining the mutation pattern.

CNVs are associated not only with the heredity form of the disease but also with the sporadic form.[15,16] So far, PD associated with rearrangements of *SNCA*, *PINK1*, and *parkin* have been described.[1,17,18] Interestingly, the severity of PD is influenced by the copy number of *SNCA*.[19] CNVs of certain unknown genes that play a pathogenic role in PD will likely be reported in the future. The copy number of these genes will possibly be important for the prediction of progression of PD. Thus, there is a

need to evaluate CNVs, taking into consideration the copy number of genes.

In conclusion, for correct determination of rearrangement mutation, mutation analysis not only in the patient but also in other family members and/or break-point analysis of genomic DNA and at the transcript level should be conducted. ■

Acknowledgments: We thank all the participants in this study. We also thank Dr. Jun Mitsui for technical advice on break-point analysis, and Ms. Yoko Imamichi for technical assistance.

References

1. Kitada T, Asakawa S, Hattori N, et al. Mutations in the parkin gene cause autosomal recessive juvenile parkinsonism. Nature. 1998;392:605–608.
2. Lücking CB, Dürr A, Bonifati V, et al. Association between early-onset Parkinson's disease and mutations in the parkin gene. N Engl J Med. 2000;342:1560–1567.
3. Nichols WC, Pankratz N, Uniacke SK, et al. Linkage stratification and mutation analysis at the parkin locus identifies mutation positive Parkinson's disease families. J Med Genet. 2002;39:489–492.
4. Lohmann E, Periquet M, Bonifati V, et al. How much phenotypic variation can be attributed to parkin genotype? Ann Neurol. 2003; 54:176–185.
5. Nuytemans K, Theuns J, Cruts M, Van Broeckhoven C. Genetic etiology of Parkinson disease associated with mutations in the SNCA, PARK2, PINK1, PARK7, and LRRK2 genes: a mutation update. Hum Mutat. 2010;7:763–780.
6. Oliveira SA, Scott WK, Martin ER, et al. Parkin mutations and susceptibility alleles in late-onset Parkinson's disease. Ann Neurol. 2003;53:624–629.
7. Kay DM, Stevens CF, Hamza TH, et al. A comprehensive analysis of deletions, multiplications, and copy number variations in PARK2. Neurology. 2010;75:1189–1194.
8. Kobayashi T, Matsumine H, Zhang J, Imamichi Y, Mizuno Y, Hattori N. Pseudo-autosomal dominant inheritance of PARK2: two families with parkin gene mutations. J Neurol Sci. 2003;207: 11–17.
9. Mitsui J, Takahashi Y, Goto J, et al. Mechanisms of genomic instabilities underlying two common fragile-site-associated loci, PARK2 and DMD, in germ cell and cancer cell lines. Am J Hum Genet. 2010;87:75–89.
10. Cesari R, Martin ES, Calin GA, et al. Parkin, a gene implicated in autosomal recessive juvenile parkinsonism, is a candidate tumor suppressor gene on chromosome 6q25-q27. Proc Natl Acad Sci U S A. 2003;100:5956–5961.
11. Marder KS, Tang MX, Mejia-Santana H, et al. Predictors of parkin mutations in early-onset Parkinson disease: the consortium on risk for early-onset Parkinson disease study. Arch Neurol. 2010;67: 731–738.
12. Abou-Sleiman PM, Muqit MM, McDonald NQ, et al. A heterozygous effect for PINK1 mutations in Parkinson's disease? Ann Neurol. 2006;60:414–419.
13. Klein C, Lohmann-Hedrich K, Rogaeva E, Schlossmacher MG, Lang AE. Deciphering the role of heterozygous mutations in genes associated with parkinsonism. Lancet Neurol. 2007;6:652–662.
14. Aten E, White SJ, Kalf ME, et al. Methods to detect CNVs in the human genome. Cytogenet Genome Res. 2008;123:313–321.
15. Blauw HM, Veldink JH, van Es MA, et al. Copy-number variation in sporadic amyotrophic lateral sclerosis: a genome-wide screen. Lancet Neurol. 2008;7:319–326.
16. Tam GW, Redon R, Carter NP, Grant SG. The role of DNA copy number variation in schizophrenia. Biol Psychiatry. 2009;66: 1005–1012.
17. Singleton AB, Farrer M, Johnson J, et al. alpha-Synuclein locus triplication causes Parkinson's disease. Science. 2003;302:841.
18. Li Y, Tomiyama H, Sato K, et al. Clinicogenetic study of PINK1 mutations in autosomal recessive early-onset parkinsonism. Neurology. 2005;64:1955–1957.
19. Fuchs J, Nilsson C, Kachergus J, et al. Phenotypic variation in a large Swedish pedigree due to SNCA duplication and triplication. Neurology. 2007;68:916–922.

nature COMMUNICATIONS

OPEN

ARTICLE

Received 12 Apr 2012 | Accepted 20 Jul 2012 | Published 21 Aug 2012

DOI: 10.1038/ncomms2016

PINK1 autophosphorylation upon membrane potential dissipation is essential for Parkin recruitment to damaged mitochondria

Kei Okatsu[1,2], Toshihiko Oka[3], Masahiro Iguchi[1], Kenji Imamura[1,2], Hidetaka Kosako[4], Naoki Tani[4], Mayumi Kimura[1], Etsu Go[1], Fumika Koyano[1,2], Manabu Funayama[5], Kahori Shiba-Fukushima[5], Shigeto Sato[5], Hideaki Shimizu[6], Yuko Fukunaga[7], Hisaaki Taniguchi[4], Masaaki Komatsu[8], Nobutaka Hattori[5], Katsuyoshi Mihara[7], Keiji Tanaka[1] & Noriyuki Matsuda[1]

Dysfunction of PINK1, a mitochondrial Ser/Thr kinase, causes familial Parkinson's disease (PD). Recent studies have revealed that PINK1 is rapidly degraded in healthy mitochondria but accumulates on the membrane potential ($\Delta\Psi$m)-deficient mitochondria, where it recruits another familial PD gene product, Parkin, to ubiquitylate the damaged mitochondria. Despite extensive study, the mechanism underlying the homeostatic control of PINK1 remains unknown. Here we report that PINK1 is autophosphorylated following a decrease in $\Delta\Psi$m and that most disease-relevant mutations hinder this event. Mass spectrometric and mutational analyses demonstrate that PINK1 autophosphorylation occurs at Ser228 and Ser402, residues that are structurally clustered together. Importantly, Ala mutation of these sites abolishes autophosphorylation of PINK1 and inhibits Parkin recruitment onto depolarized mitochondria, whereas Asp (phosphorylation-mimic) mutation promotes mitochondrial localization of Parkin even though autophosphorylation was still compromised. We propose that autophosphorylation of Ser228 and Ser402 in PINK1 is essential for efficient mitochondrial localization of Parkin.

[1] Laboratory of Protein Metabolism, Tokyo Metropolitan Institute of Medical Science, Setagaya-ku, 156-8506, Japan. [2] Department of Medical Genome Sciences, Graduate School of Frontier Sciences, The University of Tokyo, Kashiwa, Chiba 277-8561, Japan. [3] Department of Life Science, College of Science, Rikkyo University, Toshimaku-ku, Tokyo 171-8501, Japan. [4] Division of Disease Proteomics, Institute for Enzyme Research, The University of Tokushima, 770-8503, Japan. [5] Department of Neurology, Juntendo University School of Medicine, Bunkyo-ku, Tokyo 113-8421, Japan. [6] RIKEN Systems and Structural Biology Center, 1-7-22 Suehiro-cho, Tsurumi-ku, Yokohama 230-0045, Japan. [7] Department of Molecular Biology, Graduate School of Medical Science, Kyushu University, Fukuoka 812-8582, Japan. [8] Protein Metabolism Project, Tokyo Metropolitan Institute of Medical Science, Setagaya-ku, 156-8506, Japan. Correspondence and requests for materials should be addressed to N.M. (email: matsuda-nr@igakuken.or.jp).

Parkinson's disease (PD) is one of the most pervasive neurodegenerative diseases, affecting 1% of the population over the age of 65. PD commonly arises sporadically; however, in some cases the disease is familial and inherited. *PINK1* and *PARKIN* are causal genes for hereditary (that is, autosomal recessive) early-onset PD[1,2]. Studies on their functions can consequently provide important insights into the molecular mechanism of disease pathogenesis.

Although the cause of sporadic PD is likely complex, numerous evidences link mitochondrial dysfunction to its pathogenesis; for example, a moderate deficit in mitochondrial electron transport chain complex activity and mutations/deletions of mitochondrial DNA in PD patients have repeatedly been reported[3,4]. In 2008, Narendra *et al.*[5] reported that Parkin translocates to and degrades depolarized mitochondria following uncoupler treatment. Although this experimental system is an artificial one, it is commonly used as a cellular experimental model for PD that might reflect the intrinsic damage in electron transport chain and the mutations/deletions in mitochondrial DNA that inevitably lead to a decrease in membrane potential ($\Delta\Psi$m).

Newly emergent evidence has shown that PINK1- and Parkin-dependent ubiquitylation has a pivotal role in the quality control of mitochondria, which suggests that dysfunction of either PINK1 or Parkin likely results in the accumulation of low-quality mitochondria, thereby triggering early-onset familial PD. According to the most recently proposed model, selective localization of PINK1 to low-quality mitochondria facilitates the recruitment of cytosolic Parkin to the same mitochondria[6–12]. The ubiquitin ligase activity of Parkin, which is repressed under normal conditions, is re-established on damaged mitochondria[6,13]. Active Parkin then ubiquitylates mitochondrial outer membranous proteins such as Mitofusin, Miro and voltage-dependent anion channel[7,9,10,14–21]. The ubiquitylated proteins and damaged mitochondria are then degraded via the proteasome and autophagy, although the role of PINK1/Parkin in neurons remains controversial[5,19,22–25].

PD-associated PINK1 and Parkin mutations interfere with the ubiquitylation of depolarized mitochondria, suggesting the etiological importance of this process[6–9,12]. During this process, the principal initiation event is the discrimination of damaged mitochondria from their healthy counterparts. A model for this process has recently been described by Youle's group, in which newly synthesized PINK1 is imported to the inner membrane of healthy mitochondria and undergoes mitochondrial protease-dependent cleavage of its amino-terminal domain; the resulting truncated PINK1 is subsequently degraded by the proteasome[26–30]. However, because the $\Delta\Psi$m is required for import, dissipation of $\Delta\Psi$m prevents PINK1 from reaching the inner membrane. As a consequence, PINK1 remains localized to the outer mitochondrial membrane[31–33]. Although this model elegantly explains how the loss of $\Delta\Psi$m causes the accumulation of PINK1 on damaged mitochondria, the molecular mechanisms underlying PINK1 retrieval of Parkin to depolarized mitochondria remain poorly understood.

In this study, we identified two Ser residues (Ser228 and Ser402) in PINK1 that undergo autophosphorylation upon dissipation of mitochondrial $\Delta\Psi$m in cells and determined that these autophosphorylation events are imperative for the efficient retrieval of Parkin to the same mitochondria.

Results

PINK1 regulation by mitochondrial $\Delta\Psi$m. If the essence of PINK1 regulation by mitochondrial $\Delta\Psi$m is only the accumulation of PINK1, increasing the amount of PINK1 should bypass the requirement of $\Delta\Psi$m to recruit Parkin onto mitochondria. When green fluorescent protein (GFP)-Parkin and PINK1 were co-transfected in HeLa cells under the control of a strong cytomegalovirus (CMV)-derived promoter, GFP-Parkin localized on mitochondria regardless of $\Delta\Psi$m as reported previously[7]. However, the Parkin-recruitment activity of over-produced PINK1 was less than the Parkin-recruitment activity of endogenous PINK1 in the presence of the mitochondrial uncoupler carbonyl cyanide *m*-chlorophenylhydrazone (CCCP; Fig. 1a), as immunoblotting confirmed that the amount of exogenous wild-type (WT) PINK1 was much more than that of endogenous PINK1 (Fig. 1b, compare lane 1 with 3). This result indicates that endogenous PINK1 in the presence of the uncoupler more efficiently recruits Parkin to mitochondria than exogenous over-produced PINK1 in the absence of the uncoupler, and suggests that PINK1 is regulated not only quantitatively but also qualitatively in response to a decrease in mitochondrial $\Delta\Psi$m.

We next examined how aside from quantitative regulation PINK1 is regulated by the mitochondrial $\Delta\Psi$m. When HeLa cells harboring exogenous PINK1 were treated with CCCP, we realized that full-length PINK1 resolves as a doublet in immunoblots on conventional handmade 7.5% gels (Fig. 1c). The higher-molecular-weight band is rapidly observed within 30 min of CCCP treatment. This doublet is poorly resolved on commercially available precast gels (Fig. 1c), thus explaining why the doublet was not clear in our previous work[6]. Doublet formation of PINK1 is not derived from processing but rather results from post-translational modification because the molecular size of *in vitro* synthesized PINK1 corresponds to that of the lower PINK1 doublet band (Fig. 1d). To determine whether phosphorylation accounts for this modification, we performed electrophoresis using polyacrylamide gels conjugated with a 1,3-bis(bis(pyridin-2-ylmethyl)amino)propan-2-olato diMn(II) complex (referred to hereafter as Phos-tag). Phos-tag can capture phosphomonoester dianions ($ROPO_3^{2-}$) and thus acrylamide-pendant phos-tag specifically retards the migration of phosphorylated proteins, which are visualized as slower-migrating bands compared with the corresponding nonphosphorylated proteins[34]. When exogenous PINK1 was subjected to polyacrylamide gel electrophoresis (PAGE)-containing phos-tag, a clear mobility shift of full-length PINK1 was observed, suggesting that PINK1 is phosphorylated following CCCP treatment (phos-tag panel of Fig. 1c, shown by red asterisks). PINK1 phosphorylation likely involves multiple sites because two higher-molecular-weight bands are observed. We next examined whether a kinase-dead (KD) mutation (K219A, D362A and D384A) that abolishes PINK1 kinase activity[35] prevents the appearance of this phosphorylated band. To avoid the effects of endogenous PINK1, we used mouse embryonic fibroblasts (MEFs) derived from a *PINK1* knockout (*PINK1*$^{-/-}$) mouse[36] transformed with PINK1-Flag. In those cells, CCCP treatment resulted in a PINK1 doublet on a conventional 7.5% PAGE with the upper band clearly retarded in phos-tag-PAGE (Fig. 1e, asterisks in lane 2). The phosphorylated PINK1 band, however, was completely absent on both 7.5% and phos-tag PAGE in the KD mutant (Fig. 1e, lane 4), suggesting autophosphorylation. Clearer results were obtained following immunoprecipitation with an anti-Flag antibody (Fig. 1e, lanes 5–8).

We next checked whether endogenous PINK1 is also phosphorylated. As reported previously, the endogenous PINK1 signal was barely detectable under steady-state healthy conditions (lane 1 of Fig. 1f), whereas CCCP treatment promoted the emergence of endogenous PINK1 (indicated by the red asterisk in lane 2 of Fig. 1f)[6,7,37,38]. Compared with exogenous non-tagged PINK1, CCCP treatment caused endogenous PINK1 to resolve at a slightly higher-molecular weight (compare lane 2 with 3 of Fig. 1f) and its mobility was consistent with the upper phosphorylated form of exogenous non-tagged PINK1 (compare lane 2 with 4). Phos-tag PAGE confirmed that the endogenous PINK1 that accumulated following CCCP treatment is the phosphorylated form (Fig. 1f, lanes 6–8). To more convincingly demonstrate that PINK1 is phosphorylated, a mitochondrial fraction prepared from CCCP-treated cells was incubated with calf intestinal alkaline phosphatase (CIAP).

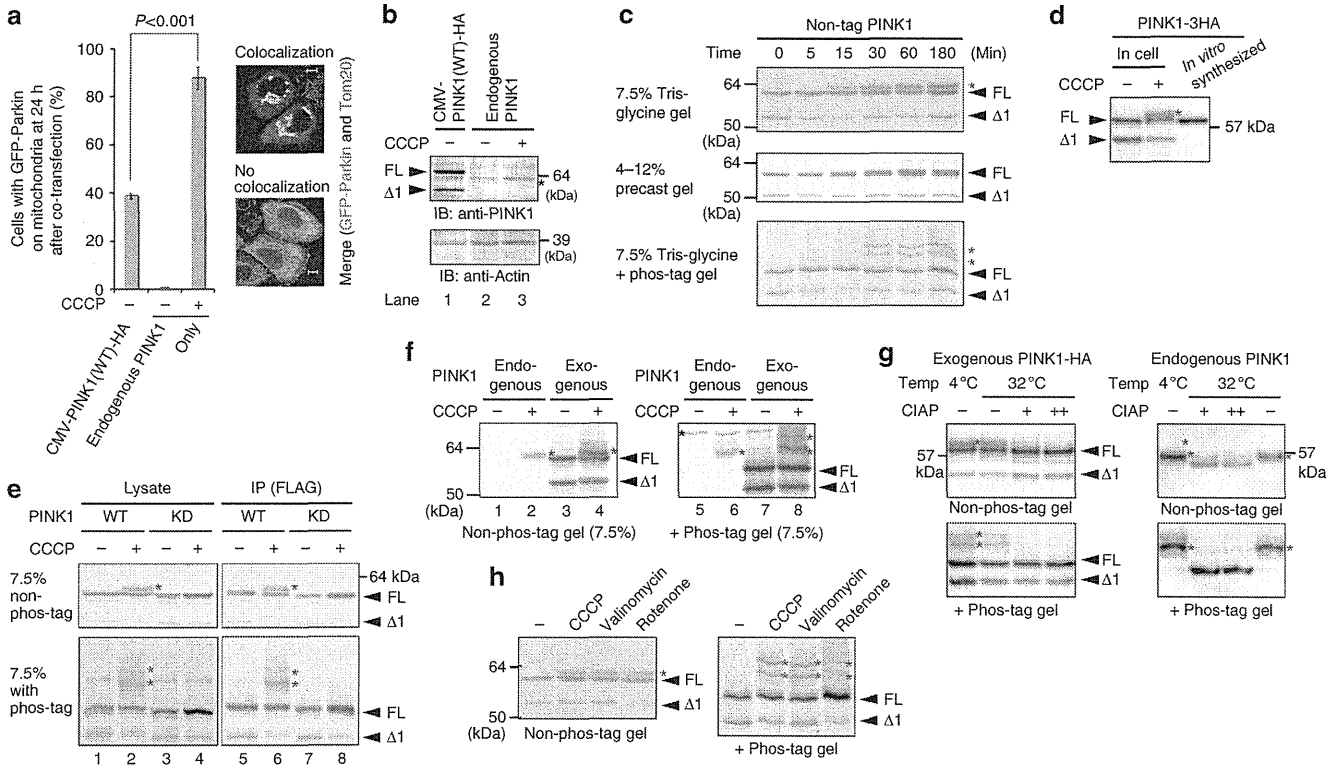

Figure 1 | PINK1 is phosphorylated following a decrease in mitochondrial $\Delta\Psi$m. (**a**) Endogenous PINK1 in the presence of CCCP (10 μM, 1 h) recruits Parkin to mitochondria more efficiently than over-produced PINK1 (CMV promoter-driven) in the absence of CCCP. The number of cells with Parkin-positive mitochondria in the Parkin-expressing cells was counted in >100 cells. Error bars represent the mean±s.d. values of three experiments. Statistical significance was calculated using analysis of variance with a Tukey–Kramer *post hoc* test. Example figures indicative of colocalization and no colocalization are shown on the right (scale bars, 10 μm). (**b**) Immunoblotting of exogenous and endogenous PINK1. The asterisk indicates the position of endogenous PINK1. Actin was used as a loading control. FL, full-length PINK1; Δ1, the N-terminal processed form. (**c**) HeLa cells expressing non-tagged PINK1 were treated with 10 μM CCCP for the indicated times and subjected to SDS–PAGE on a 7.5% Tris-glycine gel, a 4–12% precast gel or a 50 μM phos-tag containing gel. Red asterisks show phosphorylated PINK1. We routinely used HeLa cells and immunoblotting analysis was conducted with an anti-PINK1 antibody unless otherwise specified. (**d**) *In vitro* synthesized PINK1-3HA and the mitochondrial fraction of PINK1-3HA-expressing cells following CCCP treatment were subjected to immunoblotting. (**e**) The cell lysate and immunoprecipitated product of *PINK1*$^{-/-}$ MEFs-expressing WT or the PINK1 KD mutant were subjected to SDS–PAGE on a 7.5% Tris-glycine gel ±50 μM phos-tag. Red asterisks show phosphorylated PINK1. (**f**) The endogenous PINK1 in HeLa cells exists as the phosphorylated form. The black asterisk indicates a cross-reacting band and red asterisks show phosphorylated PINK1. (**g**) Phosphatase treatment caused the high-molecular shift of both exogenous and endogenous PINK1 to disappear. The mitochondrial fraction collected from HeLa cells-expressing PINK1-HA or collected from noninfected HeLa cells was treated with CIAP at the indicated temperature. Exogenous PINK1 was detected with an anti-HA antibody. + and + + mean 10 and 30 U per reaction of CIAP, respectively. (**h**) Cells expressing exogenous PINK1 were treated with CCCP (10 μM, 1 h), valinomycin (10 μM, 1 h) or rotenone (200 μM, 24 h) and subjected to SDS–PAGE on a 7.5% Tris-glycine gel ±50 μM phos-tag.

This abolished the high-molecular-weight shift of not only exogenous PINK1 but also endogenous PINK1 (Fig. 1g). PINK1 phosphorylation was also observed when cells were treated with valinomycin (another type of mitochondrial uncoupler that functions as a K^+ uniporter) or rotenone (a mitochondrial complex I inhibitor), confirming that phosphorylation is not a CCCP-specific event (Fig. 1h, red asterisks). Taken together, these results suggest that PINK1 undergoes autophosphorylation when the $\Delta\Psi$m is decreased.

PINK1 mutations can interfere with autophosphorylation. To determine whether the aforementioned event is physiologically and pathologically significant, we examined the phosphorylation status of PINK1 harboring various pathogenic mutations that cause early-onset familial PD. We studied nine pathogenic missense mutations; that is, PINK1 harboring the C92F, A168P, E240K, H271Q, G309D, L347P, G386A, G409V or E417G mutations. We also used one pathogenic mutant with an amino-acid insertion in which a CAA codon (coding for glutamine) was inserted upstream of nucleotide 1602 (cytosine) and as a result glutamine was inserted within the carboxy-terminal domain at position 534 (referred to here after as 534insQ)[39]. These PINK1 mutants were serially introduced into HeLa cells, treated with CCCP and their phosphorylation status examined. PINK1 with the C92F mutation underwent phosphorylation in a manner equivalent to WT PINK1 (Fig. 2a, lane 3). The band pattern of the G309D mutant was different from WT PINK1 in phos-tag PAGE, that is, slower-migrating bands (especially the upper band) were fainter in the G309D mutant than the WT PINK1 (phos-tag panel of Fig. 2a, lane 7). This result suggests that WT PINK1 is multiply phosphorylated whereas phosphorylation of the G309D mutant appears to be not as extensive. In the other pathogenic mutations, PINK1 phosphorylation was severely compromised (Fig. 2a) even though they localized on depolarized mitochondria (Supplementary Fig. S1). Among the pathogenic mutations, the A168P, E240K, G386A and E417G mutations are expected to perturb the Mg^{2+}/ATP-binding pocket of PINK1[40], again suggesting that phosphorylation of PINK1 is derived from autophosphorylation. We next checked the subcellular localization and autoubiquitylation

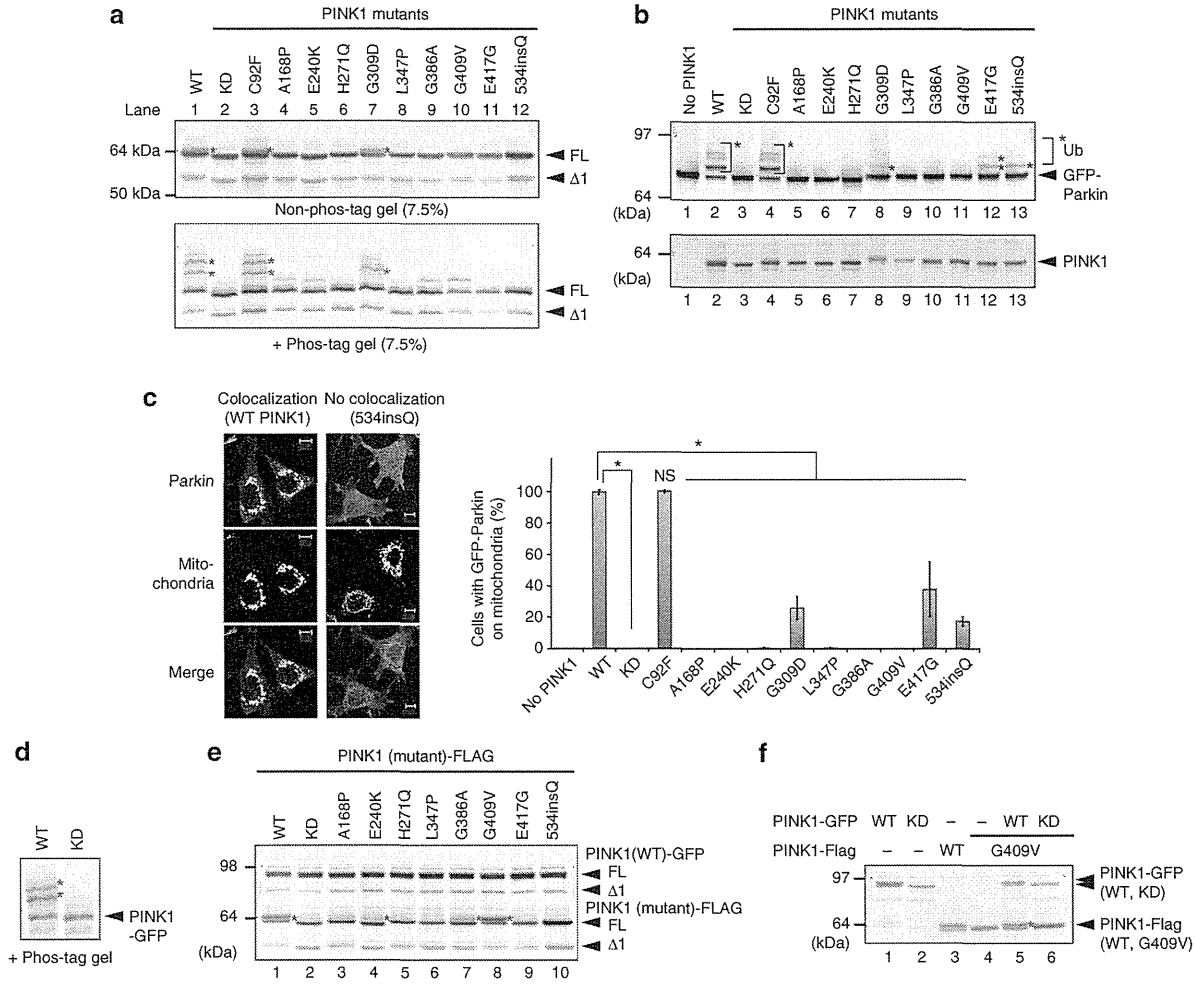

Figure 2 | PINK1 phosphorylation on damaged mitochondria is inhibited by most pathogenic mutations. (**a**) HeLa cells expressing PINK1-Flag with various pathogenic mutations were treated with CCCP, subjected to SDS-PAGE ± phos-tag and immunoblotted using an anti-PINK1 antibody. Red asterisks show phosphorylated PINK1. (**b**) *PINK1*$^{-/-}$ MEFs co-expressing GFP-Parkin and various pathogenic PINK1 mutants were subjected to non phos-tag PAGE and immunoblotting with anti-Parkin and anti-PINK1 antibodies. Blue asterisks show autoubiquitylation of GFP-Parkin, which is taken as evidence of its mitochondrial localization. (**c**) The subcellular localization of GFP-Parkin in *PINK1*$^{-/-}$ MEFs co-expressing various PINK1 mutants. Example figures indicative of colocalization and no colocalization are shown (bars, 10 μm). The number of cells with Parkin-positive mitochondria in the Parkin-expressing cells was counted in >100 cells. Error bars represent the mean±s.d. values of three experiments. Statistical significance was calculated using analysis of variance with a Tukey–Kramer *post hoc* test; *$P<0.01$; ns, not significant. (**d**) PINK1-GFP undergoes auto-phosphorylation following CCCP treatment. Red asterisks show the phosphorylated PINK1-GFP. (**e**) Various pathogenic PINK1 mutants were co-transfected with PINK1(WT)-GFP, treated with CCCP and subjected to immunoblotting using an anti-PINK1 antibody. Red asterisks show the phosphorylated bands. (**f**) HeLa cells expressing PINK1(G409V)-Flag with PINK1-GFP or PINK1(KD)-GFP were treated with CCCP and subjected to conventional PAGE. Red asterisks show phosphorylated PINK1(G409V)-Flag. FL, Δ1 and KD represent full-length PINK1, N-terminal processed PINK1 and KD mutant, respectively.

of GFP-Parkin when the aforementioned *PINK1* mutants were co-expressed in cells. We previously reported that the latent E3 activity of Parkin is activated upon recruitment to damaged mitochondria; as a consequence, autoubiquitylation of GFP-Parkin would be expected to be a good index of its mitochondrial localization[6]. In *PINK1*$^{-/-}$ MEFs co-expressing the various PINK1 mutants, only the C92F mutant exhibited autoubiquitylation of GFP-Parkin equivalent to WT PINK1 (Fig. 2b, lane 4). The G309D, E417G and 534insQ mutants showed weakened autoubiquitylation (lanes 8, 12 and 13). In contrast, the other PINK1 mutations severely hindered ubiquitylation of GFP-Parkin. Immunoblots confirmed that these mutants were expressed (Fig. 2b). Immunocytochemistry also confirmed the above results. Statistical analysis showed that co-expression of the C92F mutant resulted in the mitochondrial localization of GFP-Parkin, whereas the G309D, E417G and 534insQ mutants were unable to fully promote the mitochondrial localization of Parkin and the other pathogenic mutations failed to recruit GFP-Parkin to the mitochondria (Fig. 2c). These results showed that most pathogenic mutations compromised both the autophosphorylation activity of PINK1 and mitochondrial localization of Parkin.

We next analysed the mode of PINK1 phosphorylation. As the activity of many kinases is regulated by intermolecular interactions[41], we examined if the auto-phosphorylation of mutant PINK1 is ameliorated by co-expression with WT PINK1. When C-terminal GFP-tagged PINK1 (hereafter referred to as PINK1-GFP) was treated with CCCP and subjected to immunoblotting in the presence of phos-tag, slower-migrating phosphorylated bands were observed. These bands disappeared in the KD mutant, confirming that PINK1-GFP is functional and undergoes auto-phosphorylation

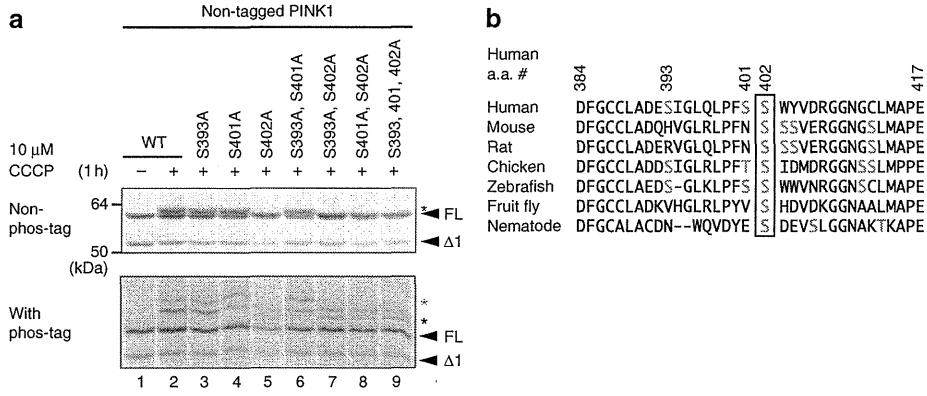

Figure 3 | S402A mutation partly inhibits the autophosphorylation of PINK1. (**a**) The S402A mutation altered the phosphorylation pattern of PINK1. PINK1 with the indicated mutations were transfected into HeLa cells and then subjected to SDS-PAGE on a 7.5% Tris-glycine gel ±50 μM phos-tag. Asterisks indicate phosphorylated PINK1 (see details of red and black asterisks in the text). (**b**) Ser/Thr residues in the activation loop of PINK1 from various organisms are shown in red font. Ser402 (boxed) is evolutionarily conserved.

(Fig. 2d). Next, PINK1-FLAG constructs harboring the various pathogenic mutations were transfected into HeLa cells with PINK1-GFP, treated with CCCP and then immunoblotted. As shown in Fig. 2e, while the majority of the mutants did not undergo phosphorylation in the presence of PINK1-GFP, a clear doublet was observed with the G409V PINK1 mutant (lane 8) and faint but reproducible doublet bands were also observed with the E240K and G386A mutants (lanes 4 and 7). Neither PINK1(G409V) alone nor co-expressed with PINK1(KD)-GFP underwent phosphorylation equivalent to WT PINK1 (lanes 4 and 6 of Fig. 2f). In contrast, PINK1(G409V) was clearly phosphorylated when WT PINK1-GFP was co-expressed (lane 5). These results suggest that autophosphorylation can occur *in trans* between two PINK1 molecules.

Ser228 and Ser402 are autophosphorylation sites of PINK1. We next sought to identify the PINK1 autophosphorylation site(s). As Ser/Thr residues in the activation loop of kinases are the most common and best-understood phosphorylation sites (for a review, see Huse and Kuriyan[42] and Nolen *et al.*[43]), we decided to focus on the PINK1 activation loop. In the case of PINK1, the region spanning amino-acid residues 384–417 (384DFG ... APE417) corresponds to the activation loop. Three Ser residues (Ser393, Ser401 and Ser402) are present within this region. We consequently exchanged these Ser residues for Ala. PINK1 with either the S393A or the S401A mutation still underwent phosphorylation in a manner similar to WT PINK1 (Fig. 3a, compare lanes 3 and 4 with lane 2). In contrast, the S402A mutation altered the band pattern of PINK1 (lane 5) with the upper band absent as assessed by conventional PAGE (non-phos-tag panel of Fig. 3a). The S402A mutation likewise affected the banding pattern on the phos-tag PAGE gel (phos-tag panel of Fig. 3a), with the emergence of a lower-molecular-weight band (black asterisk) slightly below the first band (red asterisk), which was absent in the mutation. Double and triple combinations of the S393A, S401A and S402A mutations failed to generate results that differed from the S402A mutation alone (lanes 7–9). The Ser residue at this position (402 in humans) is well conserved from mammals to nematodes, suggesting its physiological importance (Fig. 3b). The S402A mutation, however, did not impact all of the phosphorylation bands (Fig. 3a), suggesting that while S402 in the activation loop is dominantly phosphorylated, another PINK1 phosphorylation site is also utilized.

To identify the other phosphorylation site, we performed mass spectrometric analysis of autophosphorylated PINK1. Glutathione *S*-transferase (GST)-fused PINK1 was integrated into the genome of HEK293 cells by retrovirus-mediated transformation. PINK1-GST was then purified from this stable cell line following +/− CCCP treatment (Supplementary Fig. S2) and subjected to LC-MS/MS analysis after Asp-N protease digestion. A peptide equivalent to amino acids 206–230 (ERAPGAPAFPLAIKMMWNISAGSSS) was identified as a putative phosphorylated peptide. Although the unphosphorylated peptide was detected from both CCCP-treated and -untreated cells, the phosphorylated peptide was only detected from CCCP-treated cells (Fig. 4a). The MS/MS data suggested that Ser228, Ser229 or Ser230 was phosphorylated; more specific determination of the phosphorylation site is problematic (Fig. 4b). These candidate Ser residues have been relatively conserved during evolution (Fig. 4c). A peptide containing phospho-Ser402 was not identified in this analysis, possibly because the signal intensity was below the threshold of detection.

Although the three-dimensional structure of PINK1 has not yet been solved, a reliable structural model based on the structure of a related kinase (CaMKII) has been deposited in the Protein Model Database (accession code: PM0076345)[44]. Unexpectedly, we found that Ser228, Ser229 and Ser230 localized very close to Ser402 (Fig. 4d) and that they constituted a small structural patch on the surface of the PINK1 model (Supplementary Fig. S3). These Ser residues, as well as the spatially close Ser167 and Ser225, were serially exchanged for Ala. PINK1 with the S167A, S225A, S229A or S230A mutation showed double phosphorylated bands in phos-tag PAGE, although the molecular weight of those bands was altered to some degree (Fig. 4e). In contrast, the first band in phos-tag PAGE (red asterisk in Fig. 4e) disappeared in the S228A mutation (note that a faint band near the asterisk is a cross-reacting band also observed in lane 1 (WT)). Moreover, the PINK1 autophosphorylation signal was completely absent in the S228A/S402A double mutant (Fig. 4f, lane 4). Combining the S225A, S229A and S230A mutations with the S402A mutation had no such effect on the autophosphorylation signal (Fig. 4f, lanes 3, 5 and 6) and were almost indistinguishable from the S402A mutation alone (Fig. 3a, lanes 5). These results indicate that S228 and S402 are PINK1 autophosphorylation sites.

PINK1 autophosphorylation recruits Parkin to the mitochondria. Next, we sought to determine whether autophosphorylation of PINK1 is important to recruit Parkin to mitochondria. However, this experiment presents a unique challenge in that overexpression of exogenous PINK1 itself results in the targeting of Parkin to mitochondria irrespective of the mitochondrial $\Delta\Psi m$[7,45,46] and autophosphorylation (Fig. 1). We thus attempted to establish an

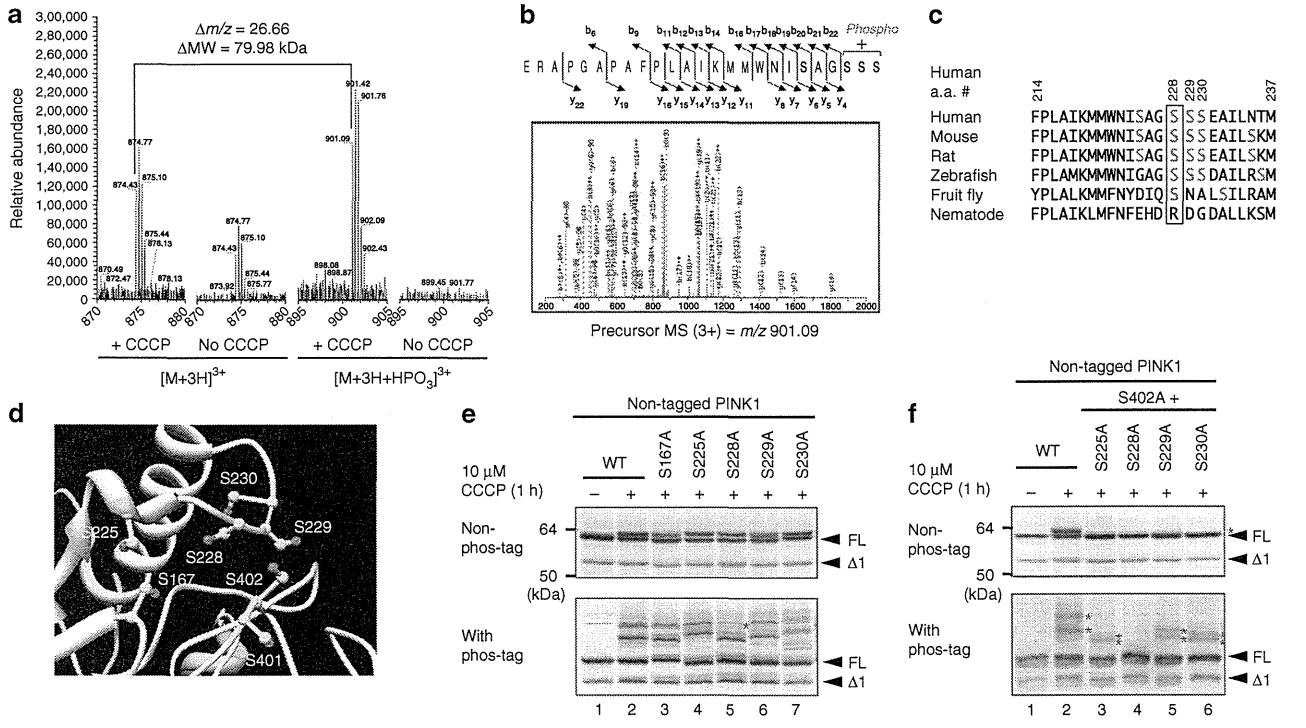

Figure 4 | S228 is another autophosphorylation site for PINK1. (**a**) *Mass spectrometric analysis of the in vivo autophosphorylation site of* PINK1. PINK1-GST purified from cells +/−CCCP treatment was subjected to LC-MS/MS analysis with a phosphorylated peptide equivalent to amino acids 206–230 detected only from CCCP-treated cells. (**b**) The MS/MS data suggested that phosphorylation occurs at Ser228, Ser229 or Ser230. (**c**) Multiple sequence alignment of PINK1 residues neighboring Ser228 from various organisms. Ser228 (boxed) has been evolutionarily conserved across most species. (**d**) Structural model (Protein Model Database ID: PM0076345) of PINK1 revealed that the possible phosphorylation sites including S228 and S402 are spatially close to one another. Ser residues are shown in yellow and hydroxyl groups are highlighted in red. (**e**) The S228A mutation changed the phosphorylation pattern of PINK1. The first band (shown by a red asterisk) in phos-tag PAGE is not observed in cell expressing the S228A mutation. (**f**) Autophosphorylation-derived signals of PINK1 in cells expressing the S228A/S402A double mutation are completely abolished. Asterisks indicate the phosphorylated form.

experimental system in which Parkin does not migrate to the healthy mitochondria even in the presence of exogenously expressed PINK1. When WT PINK1 was expressed under a strong CMV promoter, a significant amount of co-transfected GFP-Parkin was recruited to the mitochondria even without CCCP treatment (Fig. 5a, the second bar). Therefore, we modified the CMV promoter to reduce expression and found that deletion of the enhancer region in the plasmid (referred to as CMV(d1) hereafter) significantly attenuated PINK1 expression (anti-PINK1 panel of Fig. 5b, compare lane 2 with 3). With this attenuated CMV(d1) promoter, at 24 h post transfection, we observed almost no recruitment of co-expressed GFP-Parkin to mitochondria by the WT PINK1 (Fig. 5a, the third bar). We also checked the autoubiquitylation status of GFP-Parkin, a good index of its mitochondrial localization[6], and confirmed that GFP-Parkin exhibits autoubiquitylation when co-expressed with PINK1 under the control of a CMV promoter, whereas the autoubiquitylation was hardly observed with PINK1 under the control of the CMV(d1) promoter (anti-Parkin panel of Fig. 5b). Moreover, when *PINK1*$^{-/-}$ MEFs co-expressing GFP-Parkin and CMV(d1) promoter-driven PINK1 were treated with CCCP, autoubiquitylation of GFP-Parkin was clearly observed only following CCCP treatment (Fig. 5c, lane 4), suggesting that a defined expression level of exogenous PINK1 enables Parkin to localize specifically to depolarized mitochondria.

We next determined the effect of phosphorylation-deficient (Serine-to-Alanine) mutations or phosphorylation-mimic (Serine-to-Aspartic acid) mutations of Ser228 and Ser402 on Parkin recruitment. When PINK1 with either the S228A/S402A or the S228D/S402D double mutation was subjected to phos-tag PAGE, the autophosphorylation-derived PINK1 bands disappeared in both cases because the phosphorylation sites were missing (Fig. 5d). We then examined the Parkin-recruitment activity of these mutants. Importantly, the S228A/S402A mutant was unable to restore autoubiquitylation of GFP-Parkin in *PINK1*$^{-/-}$ MEFs (Fig. 5c, lane 5), whereas the S228D/S402D mutant complemented it (Fig. 5c, lane 6), although neither underwent autophosphorylation (Fig. 5d). We confirmed that the PINK1 S228A/S402A mutant localized on mitochondria following CCCP treatment as well as WT PINK1 (Fig. 5e). Immunocytochemistry of Parkin further demonstrated that the PINK1 S228D/S402D mutant promoted mitochondrial localization of Parkin equivalent to WT PINK1, whereas the PINK1 S228A/S402A mutant failed to recruit Parkin onto mitochondria (Fig. 5f,g). The results shown in Fig. 5 reveal that autophosphorylation of PINK1 is indeed important for recruiting Parkin onto damaged mitochondria, and is the first evidence that autophosphorylation of PINK1 has a crucial role in the PINK1/Parkin pathway.

Discussion

Recently, our understanding of how PINK1 and Parkin function has undergone a significant transformation that continues to evolve. We can accurately state that PINK1 and Parkin function in maintaining mitochondrial integrity by cooperatively working together to identify and label damaged mitochondria via ubiquitylation (reviewed by refs 3,31–33,47). Biochemically, Parkin functions as an E3 enzyme that catalyses the transfer of ubiquitin from E1/E2~ubiquitin to the substrate[48,49], whereas PINK1 is thought to possess Ser/Thr kinase activity. Although we and other investigators demonstrated

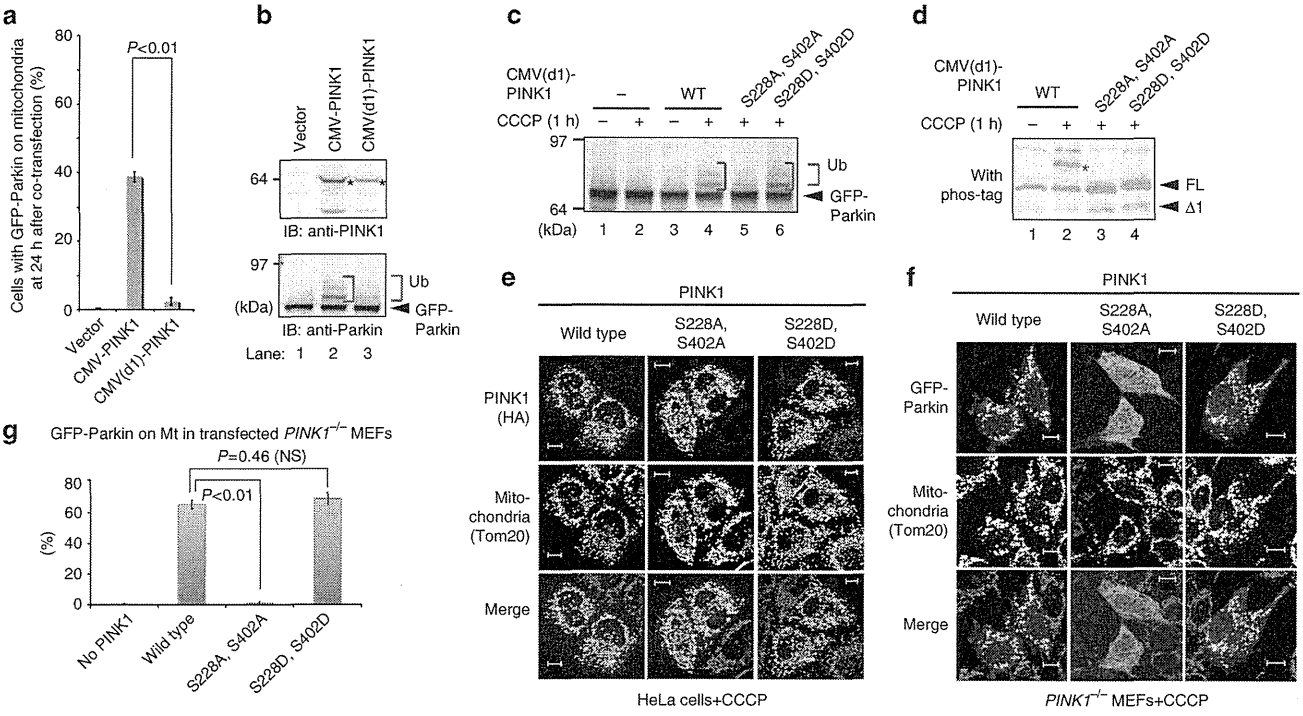

Figure 5 | PINK1 autophosphorylation of S228/S402 is essential for mitochondrial localization of Parkin. (**a**) HeLa cells were co-transfected with GFP-Parkin and CMV or CMV(d1) promoter-driven PINK1. The number of cells with Parkin-positive mitochondria was counted in >100 cells at 24 h post transfection. Error bars represent the mean±s.d. values of three experiments. Statistical significance was calculated using analysis of variance with a Tukey–Kramer *post hoc* test. (**b**) Immunoblotting with an anti-PINK1 antibody to measure the quantity of PINK1 (marked by asterisks) expressed by the CMV or CMV(d1) promoter, and autoubiquitylation activity of GFP-Parkin when the indicated PINK1 plasmids were co-transfected. The slower-migrating bands were derived from ubiquitylation (Ub). (**c**) *PINK1*$^{-/-}$ MEFs co-expressing GFP-Parkin and CMV(d1) promoter-driven PINK1 harboring the S228A/S402A or S228D/S402D mutation were subjected to immunoblotting with an anti-Parkin antibody. Ub shows autoubiquitylation of GFP-Parkin, which is taken as an indicator of its mitochondrial localization. (**d**) Both the S228A/S402A and S228D/S402D mutations hindered autophosphorylation of PINK1 in phos-tag PAGE. The asterisk indicates the phosphorylated form. FL and Δ1 mean full-length and N-terminal processed PINK1, respectively. (**e**) Subcellular localization of indicated PINK1 mutants in HeLa cells following CCCP treatment. Immunocytochemistry confirmed that both of the S228A/S402A and S228D/S402D PINK1 mutants localized on mitochondria following CCCP treatment. Bars, 10 μm. (**f**) Subcellular localization of GFP-Parkin in *PINK1*$^{-/-}$ MEFs co-expressing CMV(d1) promoter-driven PINK1 harboring the S228A/S402A or S228D/S402D mutation. Immunocytochemistry showing that the S228A/S402A PINK1 mutant disturbed the mitochondrial localization of Parkin, whereas the S228D/S402D mutant recruited Parkin to the mitochondria equivalent to WT PINK1. Bars, 10 μm. (**g**) The number of cells with Parkin-positive mitochondria was counted in >100 cells following CCCP treatment. Statistical analysis was performed as in (**a**).

that PINK1 is essential for the recruitment of Parkin to damaged mitochondria, the role of PINK1 kinase activity in Parkin recruitment remains to be fully addressed. Indeed, measurements of PINK1 kinase activity have been difficult and thus biochemical-based studies, especially *in vivo*, have not advanced enough. In this study, we addressed these problems and revealed several new findings.

The solubilization and purification of full-length PINK1 has been difficult and thus almost all studies, excluding one exception[50], of *in vitro* kinase activity have been done using a truncated PINK1 kinase domain[35,45,51–53]. Moreover, although several candidates have been reported[20,54], the physiological substrate(s) of PINK1 *in vivo* remains controversial; as a consequence the role of PINK1 kinase activity has not been fully elucidated.

In this study, we indicated that, once localized to depolarized mitochondria, PINK1 catalyses the intermolecular autophosphorylation of itself (Figs 1 and 2), although other modes of phosphorylation by another kinases cannot be ruled out completely. To study the significance of this autophosphorylation, we sought to identify the autophosphorylation site(s). Mutational analyses indicated that Ser228 and Ser402 are the PINK1 autophosphorylation sites. Moreover, direct evidence for *in vivo* phosphorylation by mass spectrometric analysis was obtained for Ser228 (Fig. 4). Although Muqit's lab[50] recently reported that insect (*Tribolium castaneum*) PINK1 catalysed autophosphorylation of Ser205 (equivalent to Ser228 in human PINK1) *in vitro*, our work provides the first direct evidence of autophosphorylation at Ser228 of PINK1 *in vivo*. Unfortunately, a peptide containing phospho-Ser402 was not identified in the MS analysis and thus the data are not as explicit as those of Ser228. However, mutational analyses suggest that both Ser228 and Ser402 are PINK1 phosphorylation sites (Figs 3a, 4e and 4f). Moreover, the PINK1 structural model predicts that these Ser residues are spatially very close and comprise a small patch on the surface, supporting the above conclusion (Fig. 4d and Supplementary Fig. S3).

It has been reported that when WT PINK1 or PINK1 continuously localized to mitochondria (OPA3-PINK1 chimera) is overexpressed in cells, Parkin localizes on the mitochondria irrespective of $\Delta\Psi m$[7,45,46]. On the other hand, autophosphorylation was not induced by over-production (Fig. 1), but did require a decrease in $\Delta\Psi m$. This result seemingly suggests that autophosphorylation of PINK1 is not important for Parkin recruitment to mitochondria. However, we propose that autophosphorylation is indeed significant for three reasons. First, based on the phosphorylation status shown in Fig. 1f,g, almost all of the endogenous PINK1 is phosphorylated in a loss of $\Delta\Psi m$-directed manner. Moreover, a majority of

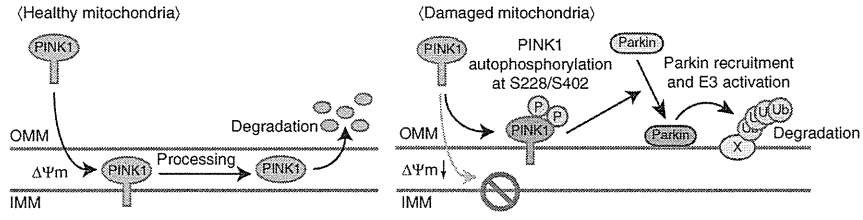

Figure 6 | A model for Parkin recruitment to the damaged mitochondria. The integrity of the mitochondria is sensed and transduced to Parkin by two sequential processes, that is the escape from membrane potential-dependent degradation and autophosphorylation of PINK1 at Ser228/Ser402. Both steps are essential for optimized Parkin recruitment and activation.

the pathogenic mutations severely compromised PINK1 autophosphorylation (Fig. 2a). Second, when the expression of exogenous PINK1 was under the control of the CMV(d1) promoter, Parkin mitochondrial localization coincided with PINK1 autophosphorylation (Fig. 5c,d). Third, a phosphorylation-deficient mutation of PINK1 (S228A/S402A) hindered the mitochondrial localization of Parkin, whereas a phosphorylation-mimic mutation of PINK1 (S228D/S402D) bypassed the necessity of PINK1 autophosphorylation for Parkin recruitment (Fig. 5c–g). Although the need for PINK1 autophosphorylation in recruiting Parkin can be suppressed by excessive over-production, we propose that PINK1 autophosphorylation under conditions such as dissipation of $\Delta\Psi$m in the presence of endogenous PINK1, or the controlled, appropriate expression of exogenous PINK1 is more physiologically relevant.

In the case of the MAP kinase extracellular signal-regulated kinase 2, its phosphorylation increases the k_{cat} by ~1,000-fold relative to the unphosphorylated form[43]. Although the physiological relevance of PINK1 autophosphorylation is unknown, we speculate that the phosphorylation of PINK1 increases the k_{cat} similar to extracellular signal-regulated kinase 2. This model is compatible with our observation described above that over-production of PINK1 suppresses the requirement of its phosphorylation.

As described in the Introduction, the basic mechanisms connecting mitochondrial damage to PINK1 accumulation have recently been elucidated[31]. The essence of the prevailing model is that PINK1 monitors mitochondrial damage via its escape from $\Delta\Psi$m-dependent import and degradation; namely, that dissipation of $\Delta\Psi$m prevents PINK1 from reaching the inner membrane, and as a consequence PINK1 remains localized to the outer mitochondrial membrane and tethered to the TOM complex[55]. However, herein we have experimentally demonstrated that while the above monitoring route is necessary for the discrimination of damaged mitochondria it might not be sufficient for fulfilling downstream events such as Parkin recruitment to mitochondria. Indeed, the low-level (but more than endogenous-level) accumulation of nonphosphorylated PINK1 on the outer membrane (for example, CMV(d1) promoter-driven PINK1(S228A/S402A) following CCCP treatment) cannot retrieve cytosolic Parkin efficiently, and autophosphorylation of PINK1 (for example, CMV(d1) promoter-driven PINK1(S228D/S402D) or endogenous PINK1 following CCCP treatment) is an essential step for optimized Parkin recruitment. We propose that the integrity of the mitochondria is sensed by the escape from $\Delta\Psi$m-dependent degradation and is transduced to Parkin via autophosphorylation of PINK1, as depicted in Fig. 6.

Methods

Plasmids. Plasmids used in this study are summarized in Supplementary Table S1. To generate the plasmid for weak PINK1 expression, the *Bgl*II–*Hin*dIII fragment within the CMV promoter was excised from pCMVTNT (Promega) and refilled with a 130-bp DNA fragment amplified using the following primers: 5′-TTGTTA GATCTCCAAAATCAACGGGACTTTCCAA-3′ and 5′-AGTGCCTCACGAC CAACTTCTG-3′ and digested with *Bgl*II and *Hin*dIII. As a result, the upstream 620 bp of the CMV promoter was deleted from pCMVTNT and the resulting plasmid was named pCMV(d1)TNT.

Cells. Various stable MEF transformants were established by infecting MEFs with recombinant retroviruses[6,56]. PINK1 and/or Parkin were cloned into a pMXs-puro vector. Retrovirus packaging cells PLAT-E[56] were transfected with the above vectors and were cultured at 37 °C for 24 h. After changing the medium, cells were further incubated at 37 °C for 24 h and the viral supernatant was collected and used for infection. MEFs were plated on 35-mm dishes at 24 h before infection, and the medium was replaced with the undiluted viral supernatant described above and 8 μg ml^{-1} polybrene (Sigma). After 2 days, transformants were selected in medium containing 5 μg ml^{-1} puromycin. HeLa cells stably expressing GFP-Parkin were established using recombinant retroviruses as well; however, as murine ecotropic retrovirus made by PLAT-E cells cannot infect HeLa cells, the retroviral receptor mCAT1 was transiently expressed in HeLa cells before viral infection. Plasmid transfection into HeLa cells and MEFs was performed using Fugene6 (Roche) and polyethylenimine (Polyscience), respectively. To depolarize the mitochondria, HeLa cells and MEFs were treated with 10 and 30 μM CCCP for 1–3 h.

Phos-tag assay and CIAP treatment. To detect phosphorylated proteins via PAGE, 7.5% polyacrylamide gels containing 50 μM phos-tag acrylamide (Wako chemicals) and 100 μM $MnCl_2$ were used. After electrophoresis, phos-tag acrylamide gels were washed with transfer buffer containing 0.01% SDS and 1 mM EDTA for 10 min with gentle shaking, and then replaced with transfer buffer containing 0.01% SDS without EDTA for 10 min according to the manufacturer's protocol. Proteins were transferred to polyvinylidene difluoride membranes and analysed by conventional immunoblotting. For CIAP treatment, a mitochondria-rich fraction (10 μg) collected by low-speed centrifugation from un-transfected or PINK1-3HA-transfected HeLa cells with CCCP treatment was incubated with 0, 10 or 30 U per reaction CIAP (Takara) for 1 h at the indicated temperature in reaction buffer (50 mM Tris–HCl pH 9.0, 1 mM $MgCl_2$, and 0.3 M trehalose), and then subjected to standard PAGE or phos-tag PAGE containing 25 μM phos-tag acrylamide (Wako Chemicals) and 50 μM $MnCl_2$ and then immunoblotted.

Immunofluorescence and immunoblotting. To detect the autoubiquitylation of GFP-Parkin by immunoblotting (IB), the cell lysate of HeLa cells or MEFs was collected in the presence of 10 mM *N*-ethylmaleimide to protect ubiquitylated Parkin from deubiquitylation. For immunofluoresecnce (IF) experiments, cells were fixed with 4% paraformaldehyde, permeabilized with 50 μg ml^{-1} digitonin and stained with the primary antibodies described below and the following secondary antibodies: mouse and/or rabbit Alexa Fluor 488, 568 and 647 (Invitrogen, 1:2,000 dilution). Cells were imaged using a laser-scanning microscope (LSM510; Carl Zeiss, Inc.). Image contrast and brightness were adjusted in Photoshop (Adobe). Antibodies used are as follows: anti-FLAG (M2 agarose; Sigma, 1:80 dilution) for immunoprecipitation, anti-actin (AC-40; Sigma, 1:1,000 dilution), anti-HA (4B2; Wako chemicals, 1:250 dilution), anti-Parkin (PRK8; Sigma-Aldrich, 1:1,500 dilution) and anti-PINK1 (BC100-494; Novus, 1:1,000 dilution) for IB, anti-GFP (3E6; Wako chemicals, 1:1,000 dilution), anti-PINK1 (BC100-494; Novus, 1:200 dilution and N4/15; NeuroMab, 1:200 dilution) and anti-Tom20 (FL-145, 1:3,000 dilution and F-10, 1:200 dilution; Santa Cruz Biotechnology) for IF. Statistical comparisons were made using analysis of variance with a Tukey–Kramer *post hoc* test in the JMP8.0.1 software (SAS Institute Inc.).

LC-MS/MS analysis of PINK1-GST. PINK1-GST from CCCP-treated and -untreated cells was subjected to SDS–PAGE and stained with CBB. PINK1-GST protein bands were excised, reduced, alkylated and digested with endoproteinase Asp-N (Roche) in 12.5 mM ammonium bicarbonate, pH 8.0, and 5 mM Tris–Cl for 16 h at 37 °C. The resultant peptides were analysed on an LTQ Orbitrap XL mass spectrometer (Thermo Scientific) with the raw data processed using Xcalibur (Thermo Scientific). The peak list files were searched against the NCBI nonredundant protein database restricted to *Homo sapiens* using the MS/MS ion search function of the Mascot search engine (Matrix Science). The 'Asp-N_ambic' enzyme parameter setting was selected for cleavage of peptide bonds N-terminally at both Asp and Glu residues.

References

1. Kitada, T. *et al.* Mutations in the parkin gene cause autosomal recessive juvenile parkinsonism. *Nature* **392,** 605–608 (1998).
2. Valente, E. M. *et al.* Hereditary early-onset Parkinson's disease caused by mutations in PINK1. *Science* **304,** 1158–1160 (2004).
3. Corti, O., Lesage, S. & Brice, A. What genetics tells us about the causes and mechanisms of Parkinson's disease. *Physiol. Rev.* **91,** 1161–1218 (2011).
4. Schapira, A. H. Mitochondria in the aetiology and pathogenesis of Parkinson's disease. *Lancet Neurol.* **7,** 97–109 (2008).
5. Narendra, D., Tanaka, A., Suen, D. F. & Youle, R. J. Parkin is recruited selectively to impaired mitochondria and promotes their autophagy. *J. Cell Biol.* **183,** 795–803 (2008).
6. Matsuda, N. *et al.* PINK1 stabilized by mitochondrial depolarization recruits Parkin to damaged mitochondria and activates latent Parkin for mitophagy. *J. Cell Biol.* **189,** 211–221 (2010).
7. Narendra, D. P. *et al.* PINK1 is selectively stabilized on impaired mitochondria to activate Parkin. *PLoS Biol.* **8,** e1000298 (2010).
8. Rakovic, A. *et al.* Effect of endogenous mutant and wild-type PINK1 on Parkin in fibroblasts from Parkinson disease patients. *Hum. Mol. Genet.* **19,** 3124–3137 (2010).
9. Geisler, S. *et al.* PINK1/Parkin-mediated mitophagy is dependent on VDAC1 and p62/SQSTM1. *Nat. Cell Biol.* **12,** 119–131 (2010).
10. Ziviani, E., Tao, R. N. & Whitworth, A. J. Drosophila parkin requires PINK1 for mitochondrial translocation and ubiquitinates mitofusin. *Proc. Natl Acad. Sci. USA* **107,** 5018–5023 (2010).
11. Lin, W. & Kang, U. J. Characterization of PINK1 processing, stability, and subcellular localization. *J. Neurochem.* **106,** 464–474 (2008).
12. Vives-Bauza, C. *et al.* PINK1-dependent recruitment of Parkin to mitochondria in mitophagy. *Proc. Natl Acad. Sci. USA* **107,** 378–383 (2010).
13. Chaugule, V. K. *et al.* Autoregulation of Parkin activity through its ubiquitin-like domain. *EMBO J.* **30,** 2853–2867 (2011).
14. Ding, W. X. *et al.* Nix is critical to two distinct phases of mitophagy, reactive oxygen species-mediated autophagy induction and Parkin-ubiquitin-p62-mediated mitochondrial priming. *J. Biol. Chem.* **285,** 27879–27890 (2010).
15. Gegg, M. E. *et al.* Mitofusin 1 and mitofusin 2 are ubiquitinated in a PINK1/parkin-dependent manner upon induction of mitophagy. *Hum. Mol. Genet.* **19,** 4861–4870 (2010).
16. Glauser, L., Sonnay, S., Stafa, K. & Moore, D. J. Parkin promotes the ubiquitination and degradation of the mitochondrial fusion factor mitofusin 1. *J. Neurochem.* **118,** 636–645 (2011).
17. Okatsu, K. *et al.* p62/SQSTM1 cooperates with Parkin for perinuclear clustering of depolarized mitochondria. *Genes to Cells* **15,** 887–900 (2010).
18. Poole, A. C., Thomas, R. E., Yu, S., Vincow, E. S. & Pallanck, L. The mitochondrial fusion-promoting factor mitofusin is a substrate of the PINK1/parkin pathway. *PloS One* **5,** e10054 (2010).
19. Tanaka, A. *et al.* Proteasome and p97 mediate mitophagy and degradation of mitofusins induced by Parkin. *J. Cell Biol.* **191,** 1367–1380 (2010).
20. Wang, X. *et al.* PINK1 and Parkin target Miro for phosphorylation and degradation to arrest mitochondrial motility. *Cell* **147,** 893–906 (2011).
21. Liu, S. *et al.* Parkinson's disease-associated kinase PINK1 regulates Miro protein level and axonal transport of mitochondria. *PLoS Genet.* **8,** e1002537 (2012).
22. Chan, N. C. *et al.* Broad activation of the ubiquitin-proteasome system by Parkin is critical for mitophagy. *Hum. Mol. Genet.* **20,** 1726–1737 (2011).
23. Lee, J. Y., Nagano, Y., Taylor, J. P., Lim, K. L. & Yao, T. P. Disease-causing mutations in parkin impair mitochondrial ubiquitination, aggregation, and HDAC6-dependent mitophagy. *J. Cell Biol.* **189,** 671–679 (2010).
24. Yoshii, S. R., Kishi, C., Ishihara, N. & Mizushima, N. Parkin mediates proteasome-dependent protein degradation and rupture of the outer mitochondrial membrane. *J. Biol. Chem.* **286,** 19630–19640 (2011).
25. Cai, Q., Zakaria, H. M., Simone, A. & Sheng, Z. H. Spatial parkin translocation and degradation of damaged mitochondria via mitophagy in live cortical neurons. *Curr. Biol.* **22,** 545–552 (2012).
26. Jin, S. M. *et al.* Mitochondrial membrane potential regulates PINK1 import and proteolytic destabilization by PARL. *J. Cell Biol.* **191,** 933–942 (2010).
27. Deas, E. *et al.* PINK1 cleavage at position A103 by the mitochondrial protease PARL. *Hum. Mol. Genet.* **20,** 867–879 (2011).
28. Shi, G. *et al.* Functional alteration of PARL contributes to mitochondrial dysregulation in Parkinson's disease. *Hum. Mol. Genet.* **20,** 1966–1974 (2011).
29. Meissner, C., Lorenz, H., Weihofen, A., Selkoe, D. J. & Lemberg, M. K. The mitochondrial intramembrane protease PARL cleaves human Pink1 to regulate Pink1 trafficking. *J. Neurochem.* **117,** 856–867 (2011).
30. Greene, A. W. *et al.* Mitochondrial processing peptidase regulates PINK1 processing, import and Parkin recruitment. *EMBO Rep.* **13,** 378–385 (2012).
31. Narendra, D. P. & Youle, R. J. Targeting mitochondrial dysfunction: role for PINK1 and Parkin in mitochondrial quality control. *Antioxid.. Redox Signal.* **14,** 1929–1938 (2011).
32. Pogson, J. H., Ivatt, R. M. & Whitworth, A. J. Molecular mechanisms of PINK1-related neurodegeneration. *Curr. Neurol. Neurosci. Rep.* **11,** 283–290 (2011).
33. Springer, W. & Kahle, P. J. Regulation of PINK1-Parkin-mediated mitophagy. *Autophagy* **7,** 266–278 (2011).
34. Kinoshita, E., Kinoshita-Kikuta, E., Takiyama, K. & Koike, T. Phosphate-binding tag, a new tool to visualize phosphorylated proteins. *Mol. Cell. Proteomics* **5,** 749–757 (2006).
35. Beilina, A. *et al.* Mutations in PTEN-induced putative kinase 1 associated with recessive parkinsonism have differential effects on protein stability. *Proc. Natl Acad. Sci. USA* **102,** 5703–5708 (2005).
36. Gautier, C. A., Kitada, T. & Shen, J. Loss of PINK1 causes mitochondrial functional defects and increased sensitivity to oxidative stress. *Proc. Natl Acad. Sci. USA* **105,** 11364–11369 (2008).
37. Zhou, C. *et al.* The kinase domain of mitochondrial PINK1 faces the cytoplasm. *Proc. Natl Acad. Sci. USA* **105,** 12022–12027 (2008).
38. Vives-Bauza, C., de Vries, R. L., Tocilescu, M. & Przedborski, S. PINK1/Parkin direct mitochondria to autophagy. *Autophagy* **6,** 315–316 (2010).
39. Klein, C. *et al.* PINK1, Parkin, and DJ-1 mutations in Italian patients with early-onset parkinsonism. *Eur. J. Hum. Genet.* **13,** 1086–1093 (2005).
40. Mills, R. D. *et al.* Biochemical aspects of the neuroprotective mechanism of PTEN-induced kinase-1 (PINK1). *J. Neurochem.* **105,** 18–33 (2008).
41. Jura, N. *et al.* Catalytic control in the EGF receptor and its connection to general kinase regulatory mechanisms. *Mol. Cell* **42,** 9–22 (2011).
42. Huse, M. & Kuriyan, J. The conformational plasticity of protein kinases. *Cell* **109,** 275–282 (2002).
43. Nolen, B., Taylor, S. & Ghosh, G. Regulation of protein kinases; controlling activity through activation segment conformation. *Mol. Cell* **15,** 661–675 (2004).
44. Cardona, F., Sanchez-Mut, J. V., Dopazo, H. & Perez-Tur, J. Phylogenetic and in silico structural analysis of the Parkinson disease-related kinase PINK1. *Hum. Mutat.* **32,** 369–378 (2011).
45. Kim, Y. *et al.* PINK1 controls mitochondrial localization of Parkin through direct phosphorylation. *Biochem. Biophys. Res. Commun.* **377,** 975–980 (2008).
46. Kawajiri, S. *et al.* PINK1 is recruited to mitochondria with parkin and associates with LC3 in mitophagy. *FEBS Lett.* **584,** 1073–1079 (2010).
47. Koh, H. & Chung, J. PINK1 and Parkin to control mitochondria remodeling. *Anatomy Cell Biol.* **43,** 179–184 (2010).
48. Chew, K. C. *et al.* Parkin mediates apparent E2-independent monoubiquitination *in vitro* and contains an intrinsic activity that catalyzes polyubiquitination. *PloS One* **6,** e19720 (2011).
49. Lim, K. L., Ng, X. H., Grace, L. G. & Yao, T. P. Mitochondrial dynamics and Parkinson's disease: focus on parkin. *Antioxid. Redox Signal.* **16,** 935–949 (2012).
50. Woodroof, H. I. *et al.* Discovery of catalytically active orthologues of the Parkinson's disease kinase PINK1: analysis of substrate specificity and impact of mutations. *Open Biol.* **1,** 110012 (2011).
51. Sim, C. H. *et al.* C-terminal truncation and Parkinson's disease-associated mutations down-regulate the protein serine/threonine kinase activity of PTEN-induced kinase-1. *Hum. Mol. Genet.* **15,** 3251–3262 (2006).
52. Silvestri, L. *et al.* Mitochondrial import and enzymatic activity of PINK1 mutants associated to recessive parkinsonism. *Hum. Mol. Genet.* **14,** 3477–3492 (2005).
53. Nakajima, A., Kataoka, K., Hong, M., Sakaguchi, M. & Huh, N. H. BRPK, a novel protein kinase showing increased expression in mouse cancer cell lines with higher metastatic potential. *Cancer Lett.* **201,** 195–201 (2003).
54. Sha, D., Chin, L. S. & Li, L. Phosphorylation of parkin by Parkinson disease-linked kinase PINK1 activates parkin E3 ligase function and NF-kappaB signaling. *Hum. Mol. Genet.* **19,** 352–363 (2010).
55. Lazarou, M., Jin, S. M., Kane, L. A. & Youle, R. J. Role of PINK1 binding to the TOM complex and alternate intracellular membranes in recruitment and activation of the E3 ligase Parkin. *Dev. Cell* **22,** 320–333 (2012).
56. Kitamura, T. *et al.* Retrovirus-mediated gene transfer and expression cloning: powerful tools in functional genomics. *Exp. Hematol.* **31,** 1007–1014 (2003).

Acknowledgements

We thank Dr. S. Yokoyama and Ms. M. Kanesaka for valuable suggestions, Dr. J. Shen for providing *PINK1*$^{-/-}$ MEF cells, Dr. T. Kitamura for PLAT-E cells, Dr. T. Iwatsubo for the PINK1 plasmid and Dr. N. Fujita for the mCAT1 plasmid. This work was supported by Grant-in-Aid for JSPS Fellows (to K.O., Grant Number 23-6061), Grant-in-Aid for Young Scientists (A) (to N.M., JSPS KAKENHI Grant Number 23687018), Grant-in-Aid for Scientific Research on Innovative Area 'Brain Environment' (to N.M., MEXT KAKENHI Grant Number 24111557), the Takeda Science Foundation (to H.K. and K.T.), Grant-in-Aid for Specially Promoted Research (to K.T., JSPS KAKENHI Grant Number 21000012) and Heath and Labor Science Research Grants (N.H. and K.T.).